


Eigenstate thermalization in an open bipartite quantum system and the semiclassical method base on correlations of adjacent local states in phase space

Chen-Huan Wu *

College of Physics and Electronic Engineering, Northwest Normal University, Lanzhou 730070, China

May 9, 2024

We investigate the eigenstate thermalization in terms of a Hermitian operator and the complex eigenkets that follows Gaussian ensemble distribution. With the non-Hermitian open bipartite system, there are, however, some global restrictions such that the elements share some of the properties of Gaussian orthogonal ensemble in diagonal and off-diagonal perspective. Such global restrictions enforce that one of the subsystem contains a nullspace with non-defective degeneracies (the primary subsystem), and the another full-ranked subsystem (the secondary subsystem). For the primary subsystem, the mixed densities in Hermitian and non-Hermitian basis exhibits global fluctuation and unidirectional (non-Hermitian skin effect) fluctuation, respectively. The former is due to the global restrictions of the whole system which plays the role of environmental disorder, while the latter is due to the nonlocal symmetries which is allowed in the restricted Hilbert space. We also investigate the integrability-chaos transition with independent perturbations in terms of the Berry autocorrelation in semiclassical limit, where there is a phase space spanned by the momentum-like projection and the range of local wave function. In a semiclassical framework, we further develop a method which is base on the correlations of adjacent local states (CALS), to investigate the integrability-chaos transition in the presence of uncorrelated perturbations and correlated integrable eigenstate fluctuations, which is applicable for both the ergodic and nonergodic systems (where the Berry autocorrelation is vanishingly small and be nearly one, respectively, similar to the characteristic of inverse participation ratio (IPR)). Also, we reveals and illustrates to a certain extent the essential role of the Golden ratio and the constant $\frac{1}{3}$ in the quantum chaos physics.

1 Introduction

In a thermalized system, the eigenstate thermalization hypothesis (ETH)[20, 21, 22, 23, 24, 26] can be verified in terms of the equality between the long-time average of a macroscopic observable with the microcanonical ensembles (diagonal ETH) and its small time fluctuation (off-diagonal ETH), which can be studied through the diagonal and off-diagonal elements of a Gaussian random matrix whose elements can be treated as random variables with zero mean and unit variance. We propose a method to constructing the commensurate eigenvector basis that are appropriate for the numerical calculation as well as the diagonal or off-diagonal ETH diagnostics. In terms of the inverse participation ratio (IPR) and normalized participation ratio (NPR), we can estimate the thermalization in reference basis of the Hilbert space with respect to the local observables. As a result of increasing number of states, the eigenstates may have diffusive superposition, in terms of the random phases and amplitudes, and then generates some coherence pattern, as well as the local conservations within the microcanonical shell. After quench, there will be two cases distinguished by the final integrable or nonintegrable systems. For the former, the environmental disorder plays the main role and leads to the global thermalization. In this case there is a unrestricted Hilbert space (with dimension D), where we assume the corresponding Hamiltonian has a degenerated bulk as is required by a globally non-Hermitian bipartite system, and the final state in a certain canonical ensemble allows the partition into D subspaces such that each one corresponds to a local macroobservable. Among all these macroobservables, they are mutually commuting, and can be viewed as the entangled thermal states that each one has a well-defined expectation (eigenvalue) from the disorder. For a collection of a full set of them, a non-Hermitian skin effect with disentangling among a common boundary of them, and in consistent with the global thermalization (or global quantum correlation), there are coherences, that does not rely on the extensive nonthermal states, happen along the direction orthogonal to where such unique (soly originates from the disorder) entanglement happen. Within each subspace, the local macroobservable with nonextensive boundary contains

*chenhuanwu1@gmail.com

also the entangling thermal states (can be regarded as a result of delocalization from the boundary with non-Hermitian skin effect), and importantly, due to the level repulsion between entangling boundaries which cause the completely depleted off-diagonal components, the coherence within each subspace will be indistinguishable over all the subspaces, or in other word, the quantum correlations in this case is allowed to freely diffusing over the whole Hilbert space. Such indistinguishability originates from fact that any coherences only happen orthogonal to the effect of disorder. Note that what we stated by completely depleted off-diagonal component here corresponds to the thermal equilibrium integrable system (free from any perturbations or prethermalizations) which means there should not be any fluctuation independent of the disorder. This phenomenon is also in consistent with the statement of Ref.[18] for a integrable final Hamiltonian, and also, what happen within each subspace can be explained by the area law scaling[10] of local states which coexist with the volume law scaling among all the subspaces (the whole Hilbert space).

This will results in increased IPR and thus enforce the states within the shell becomes localized. For the case away from the thermodynamic limit, where the dimension of the corresponding microcanonical ensemble window (which is proportional to the variance of energy density[6]) is not fixed, the reduced dimension can lower the probability to generating of coherence pattern as well as the delocalization in terms of the superpositions between eigenstates withi the shell. However, in the thermodynamic limit as required by the numerical simulation, where the variance of energy density is nearly as large as the energy density itself, we introduce below a protocol to realizing the suppression of variance of energy density as well as the coherence within the shell, which is by endowing an system-size-depdence to the range where the value of eigenstates sampled from.

The fraction of nonthermal states cause the weak ETH as well as the fluctuations, but the weak ETH will holds as long as there is a constant ratio (smaller than one) between the number of nonthermal eigenstates and that of the whole Hilbert space, in which case the fraction of nonthermal state is exponentially small in large system size limit.

By considering the second and fourth moment for the case satisfying ETH, we estimate the dependence on the system size L . The result shows that the constant $\frac{1}{3}$ as well as the Golden ratio plays a role as long as there is thermalization and non-Hermiticity (before the equilibrium). As illustrated in Supplemental material, the role of these parameters also appear in the contents of ETH diagnosis. In one-dimensional non-Abelian anyon chains[4] or the Rydberg atoms chains[3] with constrained Hilbert space, whose dimension scale as $(\frac{1+\sqrt{5}}{2})^L$ with L the system size, previous studies[3, 5] found that the number density of a single local site equals $\frac{1}{3}$, instead of the value predicted in the Gibbs ensemble with ETH, which is $(1 + (\frac{1+\sqrt{5}}{2})^2)^{-1}$. While in the method of CALS we proposed in this work, we consider several connected segments where each one of them owns an individual characteristic labeled by their derivative with the background variable set.

2 Open quantum system with global restrictions and the Loschmidt echo in Hermitian and non-Hermitian bases

For a non-Hermitian bipartite system, to guarantees the global thermalization, there is a rank-deficient subsystem (Ψ_1) which plays the main role in the Hermiticity of the global system (we thus call it the primary subsystem). The primary subsystem containing a nullspace up to $(\frac{D}{2} - 1)$ -dimensional and with non-defective degeneracies therein. We call this block the non-defectively degenerated block (NDDB). While the other subsystem (secondary subsystem) is full-rank (Ψ_2), where each eigenstate shares almost the same behavior with that in the non-degenerate region of the rank-deficient subsystem. Thus we will focus more on the rank-deficient subsystem Ψ_1 . The mixed densities base on projectors onto the eigenspaces of Ψ_1 well exhibit non-Hermiticity-enforced diffusion of quantum mutual information among all the subspaces where each one has a nonextensive boundary which can be visualized by the spectrum of Loschmidt echo.

The non-Hermitian bipartite system, despite be a open quantum system due to the complex Hilbert space, there are, however, some global restrictions such that the elements share some of the properties of Gaussian orthogonal ensemble in diagonal and off-diagonal perspective. This is realized by the elaborated complex eigenkeys (random vectors), i.e., the ingredient of the subsystems. This is like a oppoiste version of the Dyson map[17] which is mapping an original non-Hermitian system (with a subsystem structure) to a quasi-Hermitian one where some of the intrinsic non-Hermitian properties are encoded in the Hermitian one. The open non-Hermitian system encode some of the properties of the Hermitian system in Gaussian orthogonal ensemble up to second and fourth moments, where both the real and imaginary compoents participate. The real and imaginary components are correlated in eigenspace with nonzero eigenvalue and uncorrelated in nullspace. The correlated real and imaginary components can be directly seem from the biorthogonality in the non-Hermitian basis, such that $\langle \psi_{m;i} | \psi_{m;i}^* \rangle = 1$ while $\langle \psi_{m;i} | \psi_{m;i} \rangle \lesssim 1$ ($\forall i \notin NDDB$). Consistent with the joint scaling[19] of the right and left vectors.

Such global restrictions enforce that one of the subsystem contains a nullspace with non-defective degeneracies (the primary subsystem), and the another full-ranked subsystem (the secondary subsystem). For the primary subsystem, the mixed densities in Hermitian and non-Hermitian basis exhibits global fluctuation and unidirectional (non-Hermitian skin effect) fluctuation, respectively. The former is due to the global restrictions of the whole system which plays teh role of environmental disorder, while the latter is due to the nonlocal symmetries which is allowed in the restricted Hilbert space. We also investigate the integrability-chaos transition with independent perturbations in terms of the Berry autocorrelation in semicalssical limit, where there is a phase space spanned by the momentum-like projection and the range of local wave function.

Consistent with the thermaliztion with respect to the global restrictions, the two subsystems are not maximally

entangled (and thus the partial trace for $\Psi_1 \otimes \Psi_2$ over one of the subsystem is not a maximally mixed density), and in fact the two subsystems are mutually commuting in diagonal component and coherented in off-diagonal component. As also required by the non-defective degeneracies within the NDDB of Ψ_1 , the eigenstates therein is quite different from the ones with defective degeneracy (which are frustration free and can be expressed as a matrix product state). Next we define $|\Psi_1\rangle_i$ as the i -th eigenvector of Ψ_1 . The self-adjoint operators $\rho_{H;i} := |\Psi_1\rangle_i \langle \Psi_1|_i$, $\rho_{nH;i} := |\Psi_1\rangle_i \langle \Psi_1|_i^*$ can be written in the spectral decomposition form, $\rho_{H;i} = \sum_j \varepsilon_j(\rho_{H;i}) |\rho_{H;i}\rangle_j \langle \rho_{H;i}|_j$, $\rho_{nH;i} = \sum_j \varepsilon_j(\rho_{nH;i}) |\rho_{nH;i}\rangle_j \langle \rho_{nH;i}|_j$. But different to the completely localized eigenspaces like the ones in Hermitian operator H_D .

For self-adjoint operator H_D , as an integrable Hamiltonian, each eigenstate has well-defined eigenvalue and behaves as a localized state, where each one can be expressed as matrix product state and the non-defective degeneracy is absent. As a Hermitian operator, the real eigenvectors of H_D , $|E_i\rangle$ ($i = 1, \dots, D$), form a orthonormalized basis, and have many properties which are absent for the non-Hermitian operators Ψ_1 and Ψ_2 . Moreover, the basis forms two projectors $\mathcal{P}_D := \sum_{i=1}^D |E_i\rangle \langle E_i| = \mathbf{I}$, $\mathcal{P}'_D := (\sum_{i=1}^D |E_i\rangle) (\sum_{i=1}^D \langle E_i|)$. Not just the H_D itself satisfies the spectral decomposition, $H_D = \sum_{i=1}^D \varepsilon_i(H_D) |E_i\rangle \langle E_i|$, $e^{\tau H_D} = \sum_{i=1}^D e^{\tau \varepsilon_i(H_D)} |E_i\rangle \langle E_i|$, arbitrary superposition of its eigenspaces do, $\rho_D := \sum_i |H_D\rangle_i \langle H_D|_i = \sum_i \varepsilon_i(\rho_D) |\rho_D\rangle_i \langle \rho_D|_i = \dim[i] \sum_i |\rho_D\rangle_i \langle \rho_D|_i$, $e^{\tau \rho_D} = \sum_i e^{\tau \varepsilon_i(\rho_D)} |\rho_D\rangle_i \langle \rho_D|_i$. Both $|E_i\rangle \langle E_i|$ and $|\rho_D\rangle_i \langle \rho_D|_i$ are orthogonal projectors, such that, e.g., $|E_i\rangle \langle E_i| |E_j\rangle \langle E_j| = \delta_{ij} |E_i\rangle \langle E_i|$.

The imaginary part of fidelity provides a reliable criterion on judging if the system reaches the thermal equilibrium. For systems reaching thermal equilibrium (well described by generalized Gibbs ensemble), no matter it is initially consist of the integrable eigenstates where each one is protected by certain symmetry (like the maximally mixed density \mathcal{P}_D) or thermalized to a conserved Hamiltonian by some environmental disorder with volume law scaling of quantum mutual information through over all the eigenspaces under the non-Hermitian effect (like $\rho_{H;1}$), the imaginary part of fidelity always exhibits a single cluster in the evolutionary spectrum; While for the systems containing the thermal states as well as the volume law scaling entanglement entropy, the imaginary fidelity of each eigenspace as well as the whole system will exhibit splitted spectrum with more than one cluster.

2.1 Hermitian basis

For the former, the diffusion of coherences (quantum correlations) is allowed by the single symmetry sector, and thus quantum mutual information freely diffuse over the thermal states (carried by different species at a single moment) without any reflection before it vanishes in the long-time limit, which is different to the unidirectional disentangling by non-Hermitian skin effect. This corresponds to a limit of strongest disorder such that the entanglement between arbitrary macroobservables (subspaces) plays the main role, while the coherences only exist along the directions orthogonal to that of disorder. As a result of global fluctuation (as required by the generalized Gibbs ensemble; like the global magnetic fluctuation in XXZ chain with finite number of magnon species[9]), the mutual information transition along the echo spectrum boundary (by lighter carrier; like fermion charge) is system-size-dependent, and the maximal mixing as well as the maximal entanglement (also, minimal overlap) is evidenced by the fixed number of thermal states for arbitrary combinations of subspaces in Hermitian basis. During the proximity to equilibrium, the disentangling as well as the non-Hermitian-to-Hermitian transition is evidenced by the diffusive to ballistic of mutual information during which process accompanied by a maximal loss of information carrier mass. Importantly, as shown in Fig., the species at different time steps are characterized by fluctuating line-shape echo and the mesh-type echo emerges only in the continuous limit (densest time step), which preclude the carrier risen by nonlocal symmetries (like the heavier quasiparticle) in the case of non-Hermitian basis which violates the generalized Gibbs ensemble. The line-type echo for each species (or bound states, which are definite with respect to the disorder) exhibit mainly the fluctuation instead of thermalization.

Specifically, despite there is non-Hermitian skin effect along each direction where coherence happen, the disentangling effect is infinitely diluted by the subspaces of NDDB such that each subspaces out of NDDB behaves purely local instead of quasi-local (for a case of quasi-local see Ref.[9]). This is also the reason why any coherence as well as nonlocal symmetry is precluded and making sure that all the emergent species is governed by the environmental disorder.

As shown in Fig., the role of NDD subspaces here is to homogenize the information transport of a certain species.

Collecting all the subspaces in Hermitian basis results in a line-type echo $\mathcal{L}(\rho_{H;1})$, which implies that completely merged echo spectrum corresponds to a Hermitian state and equivalents to the final integrable state of each subspace. Similarly, by setting different time intervals the mesh-pattern spectrum can be decomposed into multiple line-shape patterns, where different time intervals correspond to different frequencies (or effective temperatures when one introducing the generalized Gibbs ensemble to here), and distinct frequencies (even very close) will not overlap in echo spectrum which reflecting the level repulsion between the entangling nonintegrable states. To illustrate such decomposition of echo spectrum, we always plot the spectrum in narrowest time step (ideally the highest energy one) by blue, while the other arbitrary time steps by other colors.

Each line-type echo corresponds to a local fluctuating state which arrives the thermal equilibrium of a generalized Gibbs ensemble at a certain effective temperature when the fluctuation vanishes, and it is differentiable everywhere. Also, the fluctuating amplitude is solely determined by the upper and lower boundaries of the whole echo spectrum, where $\partial_t \mathcal{L}_{\text{line}} = 0$. This well match the orthodox picture for a hermitian system where interaction effect between delocalized subsystems is absent (which, however, plays a key role in non-Hermitian basis). The local character (continuous everywhere) of line-type echo prohibits the nonintegrability and chaos, where there is large fluctuations before equilibrium. Such large fluctuation is consistent with, e.g., the binary nature of the disorder[10], where the interactions and (disorder-free) nonthermal states are prohibited.

As each subspace of Hermitian basis is a local state with respect to the global equilibrium Hermitian system $(\rho_{H;c_1})$ where only conservation is attributed by the disorder, there is indeed an indistinguishability[11] between the maximally mixed state and the pure state. The maximally mixed state can be a result of the maximal entanglement, which can be expressed as a reduced state by tracing over part of the entangled states. Consistent with the feature of mixed-state nature, $|\text{Tr}[\rho_{H;i \notin NDDDB}^2]| \lesssim 1$, each subspace as well as arbitrary combination will not coherently combine with others such that there is diffusive quantum mutual information (or correlation) carried by the heavier information carrier and definite (system-size-dependent) mutual information carried by the lighter carrier, and both the fluctuations here are dynamical and global due to the absence of nonlocal symmetries. Also, each subspace in Hermitian basis $\rho_{H;i \notin NDDDB}$ (complex symmetry matrix) is not a Hermitian matrix, and $e^{i\rho_{H;i \notin NDDDB}t}$ is not unitary and the Frobenius norm $\|e^{i\rho_{H;i \notin NDDDB}t}\|$ is time-dependent.

2.2 non-Hermitian basis

For the latter case, there is always the coherences which result in distinct symmetry sectors between which hinder the diffusion of quantum correlations (or coherences) throughout the whole system and thus prohibits the volume law scaling of quantum mutual information, and the whole system cannot be partitioned into mutually commuting (but entangled) macroobservables. The observables therein that coherently combine with others are always extensive, and it is unavailable to find a complete set of coherence such that the resulting system be nonextensive. In this case, the diminished entanglement entropy due to the non-Hermitian skin effect happens periodically during the evolution, and such coherences happen along the direction of disorder usually generate complex patterns during the relaxation, and there are indeed the off-diagonal components that participate which cause the random states (mutually less overlapped; while the perfect) with exponentially large Hilbert space. This emergent role of off-diagonal component during this process is similar to the interacting particles with distinct energies generate quasiparticles with new energy with the energy here in analogy with the periodicities during the evolution. Thus there is a restricted Hilbert space for the initial states with persistent initial state recurrence. Specifically, except the NDD regime which is completely disorder-free, there are disorder-independent coherences by the disorder-free nonlocal symmetries, each mesh-pattern echo contains nonthermal states and is extensive. As a result, there are repeated mergings in the echo spectrum, since the preserving nonthermal states always have finite response to a larger nonlocal conservation (or larger squeezed generalized Gibbs ensemble[9]). The coherence-induced thermal relaxation is always unidirectional (or local) due to the non-Hermitian skin effect.

Different to the subspaces in Hermitian basis, each subspace in non-Hermitian basis $\rho_{nH;i \notin NDDDB}$ is a (complex) Hermitian matrix and has $\text{Tr}[\rho_{nH;i \notin NDDDB}] = \text{Tr}[\rho_{nH;i \notin NDDDB}^2] = 1$, thus it behaves more like a pure state which reflects its intrinsic initial-state-fidelity, and specifically, for the full-rank one $\rho_{nH;c_1}$, its exponential form factor $e^{i\rho_{nH;c_1}t}$ is isometric and unitary, thus $e^{i\rho_{nH;c_1}t} \in \text{GL}(\mathbf{B})$ with \mathbf{B} the complex Banach space such that $\rho_{nH;c_1} \in \mathbf{B}$.

Consequently, a thermal equilibrium-required effective temperature for the generalized Gibbs ensemble is ill-defined, for the disentangling induced by non-Hermitian skin effect. The preserving nonthermal states after coherences generate extensive echo spectrum, and as a significant feature of non-Hermiticity, each mesh-pattern echo with diffusion of mutual information has singularities with $\partial_t \mathcal{L} = \infty$ (or $\lim_{t \rightarrow \infty} \mathcal{L} = 0$ according to our ansatz in Supplementary material). As we illustrate below, such singularities are a reliable sign for the existence of non-Hermiticity and delocalized states (according to CALS, the zero limit $\lim_{t \rightarrow \infty} \mathcal{L} = 0$ enforces $\partial_{t^+} = \partial_t$, distinct from the result of a final Hermitian system).

The localization through coherence cannot induce the Hermitian-type equilibrium and disentangling, but only results in the discontinued disentangling. This can be directly seen from the Loschmidt echo spectrum where there are irregular boundaries with drastic fluctuations caused by the non-Hermiticity-induced instability and the diffusion of quantum mutual information, until the periodically appearing merging which happens in the moments of thermal equilibrium and with the complete reflection of quantum mutual information (change the carrier, e.g., from fermions to spin[10]). In non-Hermitian basis with distinct left and right vectors, it is impossible to obtain a completely localized Hermitian system but an extensive one, which, however, is still possible to be partitioned into entangled subspaces whose corresponding periodicities guarantee they can be nested in an incoherent way (will not generate any off-diagonal components). A typical example is the $\rho_{nH;c_2}$ and $\rho_{nH;c_3}$ which are local subspaces with respect to $\rho_{nH;1}$. As a result, the imaginary fidelities exhibit a single cluster in the evolution.

As shown in Fig.2, the spectrum can be decomposed into mesh-type echoes in larger time intervals and each species (unless the one in the densest time interval) does not have to be the same in different delocalized states. In terms of these mesh-patterns that close over the delocalized states, there is a third way for the transition of quantum mutual information other than the ways with the same degree of ergodicity over all the delocalized states (like the above-mentioned area law scaling by light information carrier and volume law scaling by heavy information carrier).

As shown in , the coherence between subspaces in non-Hermitian basis outside the NDDB originates from their imaginary part of Loschmidt echo, where the delocalization happens whenever the thermal states therein (both have degrees-of-freedom along the direction of disorder) form a disentangling effect through the coherence, and at those moments the quantum mutual information must be reflected by a certain component. Obviously, the localization (disentangling) discussed here is of the exponential-type and related to the exponentially increased Hilbert space dimension away from the disentangling boundaries which is necessary to allowing the quantum mutual information to diffuse through over the obstructions between the previous delocalized states.

The subspaces $\rho_{nH;i \notin NDDDB}$ also correspond to a set of local projection operators (Hermitian matrices) such that their arbitrary combinations take exactly zero expectation value on that of the NDD states, $\rho_{nH;c_2}|\rho_{NDD;c}\rangle = 0$, which shares the similar anomalous properties of target states in Ref.[12] and is consistent with the nonfluctuating local character for the nonthermal states in NDDB. The ETH is violated as the vanishing of initial state fidelity causes a dynamical

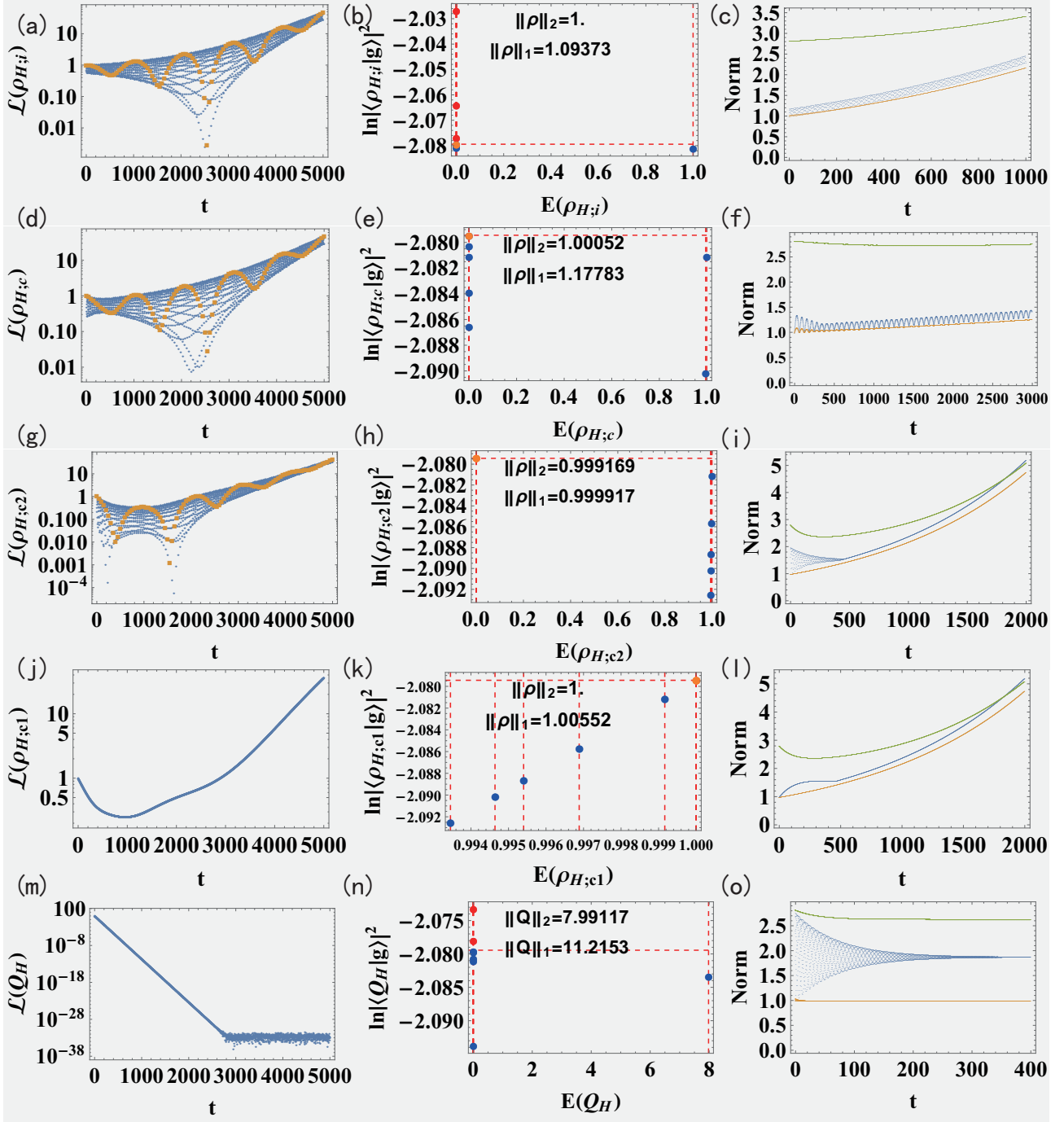


Figure 1: (a) The Loschmidt echo in Hermitian basis. (b) The overlap between eigenstates of $\rho_{H;i}$ with the chosen ground state, which, by definition, allows the cluster decomposition. The larger the overlapping with ground state, larger the initial state fidelity and lower the effect from disorder. The thermal state with low overlap with ground state ($< \frac{1}{D}$) are labelled by blue circle, the state at overlap $\frac{1}{D}$ is labelled by orange circle. The non-thermal states with high overlap with ground state ($> \frac{1}{D}$) are labelled by red circle. The vertical dashed lines label the positions of the real part of eigenenergies of $\rho_{H;i}$. Similar representation in log scale is used in Refs.[15, 16]. (c) The blue, orange, and green label the 1-norm, 2-norm, and Frobenius norm of $e^{i\rho t}$ with ρ the corresponding density.

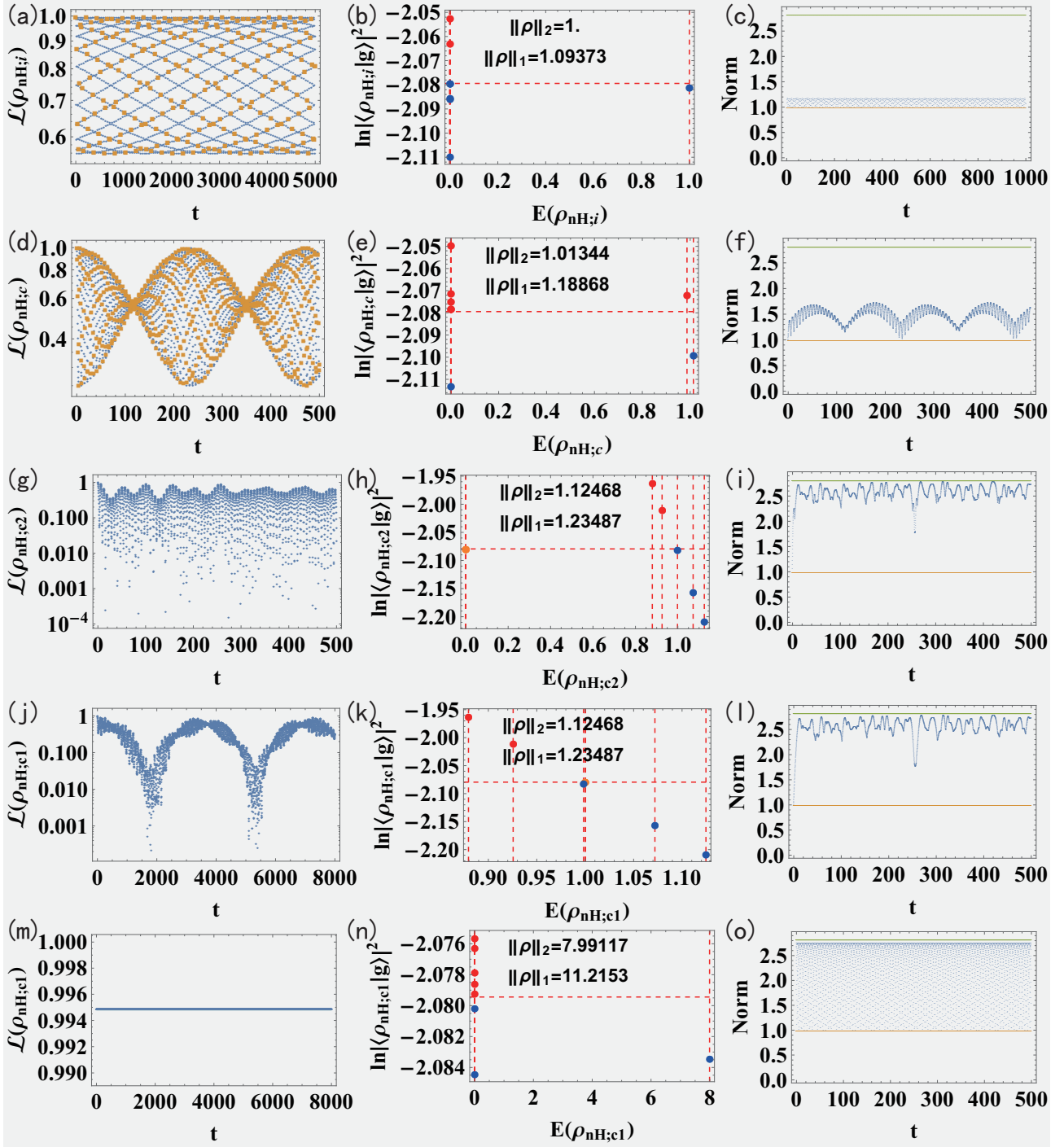


Figure 2: The same with Fig.1 but for non-Hermitian basis.

mode instead of a static microcanonical ensemble result, and the fail of thermalization for non-Hermitian basis is in consistent with the squeezed generalized Gibbs ensemble of Ref.[9]. The periodic spectrum with repeated delocalized states originates from the maximal chaos within each delocalized state which involving all the possible weights for the nested mesh-patterns.

2.3 Comparasion for the two bases

In terms the Loschmidt echo, the effect of environmental disorder on the subspaces can be visualized by a mesh-patterned spectrum merging to a line during (unitary) time evolution, during which process the entanglement entropy changes from volume-law scaling (proportionally to the bulk size of subspace) to the area-law scaling (proportionally to the spectrum upper boundary), and this reflects the thermalization to generalized Gibbs ensemble. This happen for the Hermitian basis, and the merged line-shape echo in long time can be refered to the local ground state which will not hinder the thermalization (Hermiticity) of the full system. While in non-Hermitian basis with non-adiabatic evolution, the proximity to area-law scaling is due to the coherence-induced delocalized mode, which emerges discretically in the echo spectrum (quanta of the bound states). Such delocalized modes is the origin of initial state fidelity, and can be realized by the quanta of global magnetization in XXZ Heisenberg chain[9] and unconserved number of (resonance-induced) excitations in hard-core Bose-Hubbard lattice[13]. In both bases, the arbitrary combinations of NDD subspaces behave free from the disorder.

The presence (absence) of nonlocal symmetries in non-Hermitian basis (Hermitian basis) corresponds to a vanishing (finite) long time susceptibility of the mutual information carrier. As an example, for charge susceptibility, which is finite in thermalization case, there will be nonvanishing charge cumulant which is well described by high order functional derivative[9] (the order is determined by the precision that the global conservation be considered). This is in agree with our theory that the emergence of nonlocal symmetry is signaled by the cutoff on the order of functional derivative, while the preserved derivatives upto infinite order, as shown in Eq.(43) in Appendix.B, always corresponds to the thermalization case.

In summary, the forward-scattering structure[15, 16] of the eigenstates within NDDB leads to the result which is necessary for the non-defective degeneracies, that is, arbitrary combinations of subspaces therein will not cause any biased effect and behave as the separable (disorder-free) pure states. This is due to the infinitely large dimension of effective Hilbert space (in terms of the eigenvalues therein down to log scale) attenuate the effect of off-diagonal component such that the initial-state-related polarization is able to be preserved. While the incompletely attenuated off-diagonal component (despite the exponentially growth of Hilbert space dimension) plays a significant role outside the NDDB in non-Hermitian basis, which is the ingredient of the disorder-induced fluctuations. The biased (through the coherence in the echo boundary) effect induced by the coupling between extensive subspaces is unique phenomenon in the part outside the NDDB in non-Hermitian basis, during which process the periodic disentangling patterns emerge as can be seem from the periodic merging in echo spectrum. These periodic mergings correspond to the moments with (coherence-induced) unit initial-state-fidelity, which are free from disorder and correspond dynamically to the discontinued Krylov subspaces (unlike its continuous counterpart in the nullspace). Thus the role of off-diagonal component in non-Hermitian basis is to obtain an effective Choi matrix isomorphically mapped by a linear map up to infinite size.

As shown in the middle column of Figs.1,2, the logarithm of the overlaps between mixed density eigenstate and ground state are folded along the real eigenenergies, except for the densities $\rho_{H;c_1}$, $\rho_{nH;c_1}$ and $\rho_{nH;c_2}$ where there is a linear nondegenerated band. The common feature of these densities is the suppressed thermalization through the global fluctuation (for $\rho_{H;c_1}$) or non-Hermitian skin effect (for $\rho_{nH;c_1}$ and $\rho_{nH;c_2}$). Thus the disentangling with the disorder participated attribute to unfold the information of the complex band in terms of the real eigenenergies. While the ability for the imaginary part to holding the informations about the non-Hermiticity has been widely proved, e.g., through the quasiparticle lifetime[18].

Note that, the Loschmidt echo here provides a simply and intuitive way to estimate the effect of disorder and the remanent initial properties. The memory of initial state is encoded by the ground state which is the summation over all eigenstates of the primary subsystem. This selected ground state has a perfect performance in access the ground properties. In contrast to the ingredient of the restricted bipartite system (the complex eigenkets), the eigenstates of each subsystem (mainly the primary one) intrinsically carrier the invariant property that free from the environmental disorder. This is a much convinient process to access a state exhibits perfect ground property, compares to, e.g., the variational monte carlo method[19], where the expansion coefficients of a singlet ground state require ergodically sample all the possible bonding amplitudes (to realize a global invariance independent). While our method here dexterously overcome this difficulty. This is more convinient for the current case compares to the quantum fidelity, where the overlaped states are distinkted by the complex (nonreciprocity-dependent) dynamical parameter and the phase transition is rapidly finished near the quantum criticality. The Loschmidt echo provides a tool to observe the slow proximity to the localized state (or back to the delocalized one), with the real time be the parameter.

3 System size dependence

To revealing more properties of the complex eigenvectors (ingredient of our closed bipartite system with complex Hilbert space) that exhibit unusual GOE statistical results, we next focus on the system-size dependence for the second and fourth moment of these complex eigenvectors. We randomly sample L times from $\frac{1}{\sqrt{D}}\langle\psi_{m;i}|\psi_{m;i}\rangle$ ($i = 1, \dots, D$),

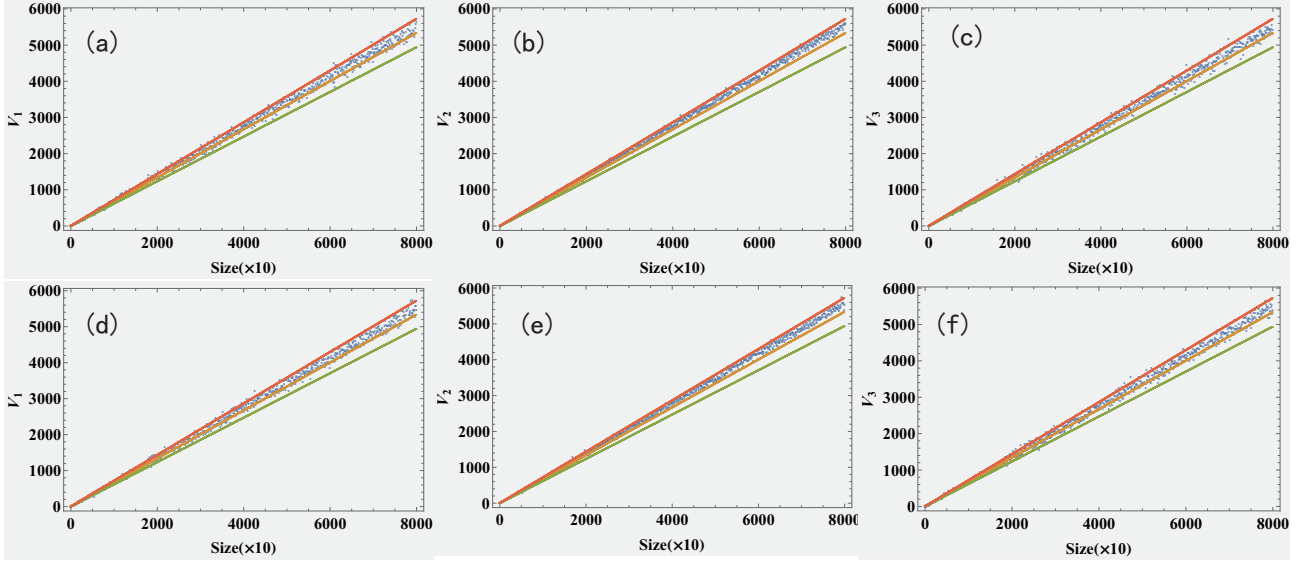


Figure 3: The Eq.(1) is represented by the blue dots. The orange, green, and red lines are $\frac{2}{3}L$, $(\phi_g - 1)L \approx 0.618L$, and $(\frac{2}{3} + \eta_g)L \approx 0.715L$, respectively.

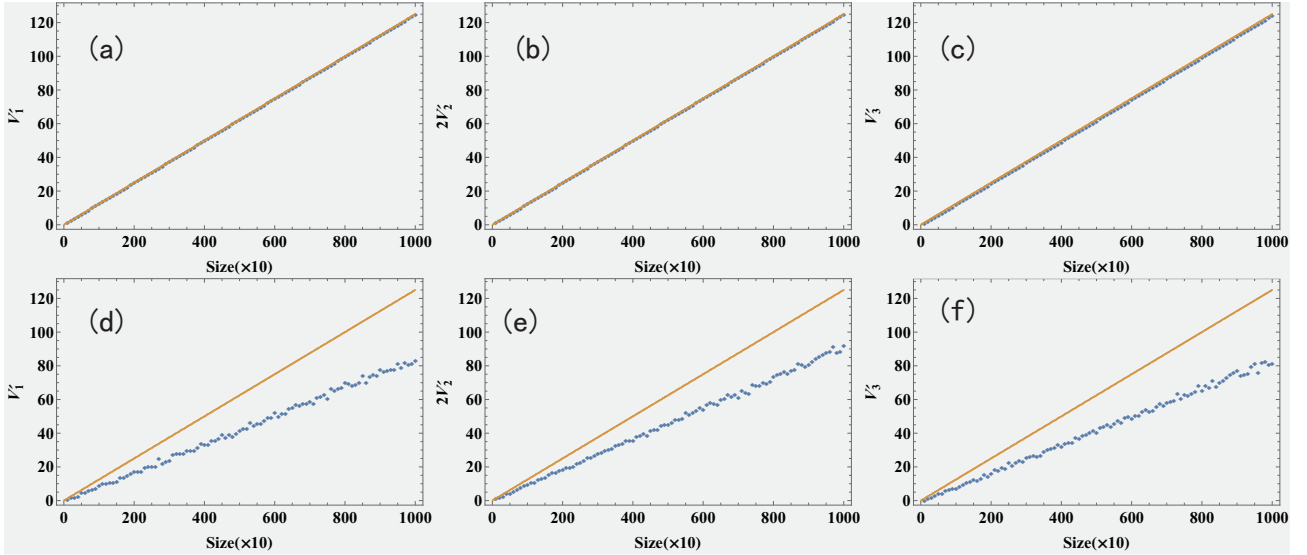


Figure 4: The orange line is $\frac{L}{D}$.

and estimate the following expressions

$$\begin{aligned}
 V_1(L) &= \frac{1}{L} \left(\sum_{i; \dim i=L} \frac{1}{\sqrt{\mathcal{C}}} |\langle \psi_{m,i} | \psi_{m,i} \rangle|^2 \right), \\
 V_2(L) &= \frac{1}{2} \left(\sum_{i; \dim i=L} \frac{1}{\mathcal{C}} |\langle \psi_{m,i} | \psi_{m,i} \rangle|^2 \right), \\
 V_3(L) &= \frac{1}{L} \left(1 - \sum_{i; \dim i=L} \frac{1}{\sqrt{\mathcal{C}}} |\langle \psi_{m,i} | \psi_{m,i} \rangle|^2 \right),
 \end{aligned} \tag{1}$$

where the factor $\mathcal{C} = \sum_{i,j=1}^D |\langle \psi_{m,i} | \psi_{m,j} \rangle|$ is determined by the primary subsystem. Then as a result of thermalization, we found that $(\frac{2}{3} + \eta_g)L > V_i(L) > \frac{2}{3}L$ ($i = 1, 2, 3$) where $\eta_g = \frac{2}{3} - (\phi_g - 1) \approx 0.04867$ is the constant determined by the Golden ratio ϕ_g .

The above results are in contrast to those without the thermalization, where we found that $V'_1(L) = 2V'_2(L) = V'_3(L) = \frac{1}{D}L$. Here $V'_i(L)$ are nothing but replacing the $\psi_{m,i}$ in Eq.1 by $\Psi_{m,i}$ (the eigenvectors of the built subsystems). The strictly homogenized result for arbitrary system size reflect a integrable scenario, in which case the constant $\frac{1}{3}$ and Golden ratio play no role, and in agree with the system without thermalization.

We also shown in Fig.5 the corresponding inverse participation ratio (IPR), i.e., the ratio between fourth moment and

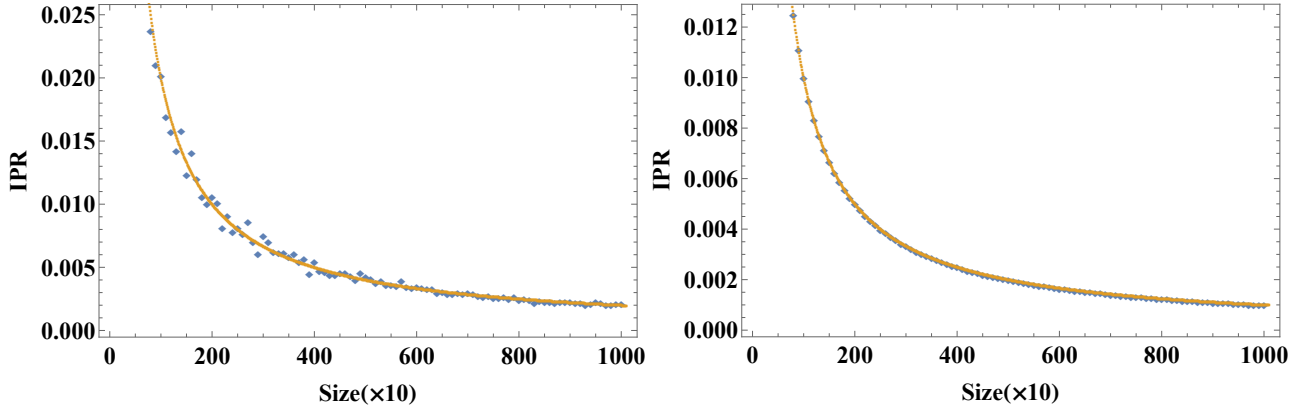


Figure 5: IPR for the states sampled from $\psi_{m;i}$ (left) and $\Psi_{m;i}$ (right). The solid lines are $2L^{-1}$ and L^{-1} in left and right panels, respectively.

squared second moment, for the states sampled from $\psi_{m;i}$ and $\Psi_{m;i}$, where both satisfy $IPR \sim L^{-1}$ and thus implying the local character. That means, for $\psi_{m;i}$, despite the nonlocal symmetry, it still satisfies the prediction of ETH (as long as the $V_i(L)$ exhibit a roughly linear distribution on size L), and this meets the case of Hermitian basis as we discuss in above section.

Comparing $V_i(L)$ and $V'_i(L)$ as well as the corresponding IPR for the states sampled from $\psi_{m;i}$ and $\Psi_{m;i}$, the thermalization only exist for the former which is attributed by the off-diagonal fluctuation and such fluctuation is weaker for the fourth moment ($V_2(L)$) compares to the second moment ($V_1(L)$ and $V_3(L)$). The nonlocal symmetry results in the emergent role of $\frac{1}{3}$ and Golden ratio, which directly reveals the existence of restricted Hilbert space. Also, the primary and secondary subsystems share the same size-dependence for $V_i(L)$ (especially the same normalization factor \mathcal{N}), which in agree with the character of the bipartite closed system, i.e., the diagonal (off-diagonal) components of the two subsystems are uncorrelated (correlated). Such local symmetry (satisfies the ETH) is absent in terms of $V'_i(L)$, where for the primary subsystem the ensemble-dominated behavior is absent, and for the secondary subsystem it is dominated by non-local symmetry (violate ETH). This is also the precondition to explore the global fluctuation (GGE) and the unglobal fluctuation (SGGE) in terms of the mixed states base on $\Psi_{m;i}$'s, as shown in Sec.2.

4 Integrability-chaos transition in terms of the Berry autocorrelation in semiclassical limit

The integrable system eigenstate basis can be expressed by a operator in power of good quantum number acting on vacuum state. Such operator usually form the generator with its conjugate. A weak perturbation may modify the good quantum number in an noninteracting integrable system. In semiclassical limit, using Berry conjecture, the noninteracting integrable eigenstates can be casted into the action corresponding to different good quantum numbers, where each action corresponds to a torus in the classical phase space. While for the interacting system, the integrable eigenstates are the superpositions of different good quantum numbers (or different torus).

The autocorrelation given by the Berry conjecture in terms of the perturbations V_1 and V_2 reads

$$\mathcal{C}(r_i, q) = \frac{\overline{V_1(q + \frac{r_i}{2})V_2(q - \frac{r_i}{2})}}{V_1(q)V_2(q)}, \quad (2)$$

where q denotes the length of local wave functions of the two perturbations, and r_i denotes the one-body density fluctuation. The numerator of $\mathcal{C}(r_i, q)$ is the averaged Wigner function (the average is taken over all possible \mathbf{p} and q),

$$\overline{V_1(q + \frac{r_i}{2})V_2(q - \frac{r_i}{2})} = \int d\mathbf{p} e^{-i\mathbf{p}\cdot\mathbf{r}_i} \int d\mathbf{r}_i e^{i\mathbf{p}\cdot\mathbf{r}_i} V_1(q + \frac{r_i}{2})V_2(q - \frac{r_i}{2}), \quad (3)$$

where the large fluctuation effect of the integrable eigenstates is smoothed out by the ensemble average. As shown in Fig.6, the momentum-like variable \mathbf{p} corresponds to the projection, and the coordinate-like variable \mathbf{q} corresponds to the range of local wave functions. In the nonintegrable limit, where the length of \mathbf{p} is large, we can neglect the \mathbf{p} -dependence of the autocorrelation; While when close to the caustic point (the integrable limit), the range-dependence can be neglected. The denominator of \mathcal{C} is the local average probability density (i.e., the Wigner distribution of a pure-state-like single-particle density),

$$V_1(q)V_2(q) = \int d\mathbf{p} \int d\mathbf{r}_i e^{i\mathbf{p}\cdot\mathbf{r}_i} V_1(q + \frac{r_i}{2})V_2(q - \frac{r_i}{2}). \quad (4)$$

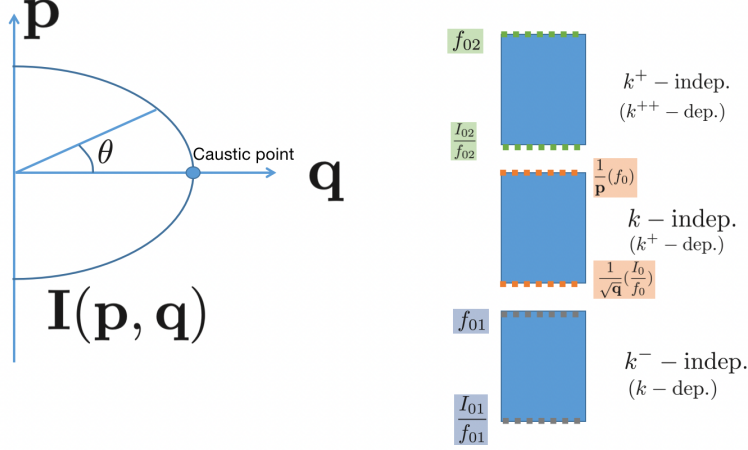


Figure 6: (Left) Schematic diagram for the phase space[4] where $I(\mathbf{p}, \mathbf{q})$ is a classical action. (Right) The segments for the method CALS where k is the variable in centroid here.

The reason for such differences between the denominator and numerator is the special selections in the numerator, through the actions in the classical phase space $\mathbf{I}(\mathbf{p}, \mathbf{q})$, where \mathbf{p} is direction that the averaged Wigner function projects to the averaged probability density function.

The correlation $\mathcal{C}(r_i, \mathbf{q})$ directly reflect the whole picture of system: The strictly Hermitian case where the system reaches thermal equilibrium, corresponds to $\mathcal{C}(r_i, \mathbf{q}) = 1$ for arbitrary large local lengths \mathbf{q} (such that all densities are exactly the same) under the condition $r_i = 0$ (equivalents to the caustic point) and with the unspecified (\mathbf{p}, \mathbf{q}) , where the action of torus $\mathbf{I}(\mathbf{p}, \mathbf{q})$ in phase space fail to dominate the average Wigner distribution. For finite value of r_i , there is a integrability-chaos transition and the system move toward the nonintegrable side with the reduced r_i . There is a minimal $r_i (\neq 0)$ where the system reaches strongest nonintegrability, and this corresponds to the density $\rho_{nH;c_2}$ with largest periodicity in the echo spectrum due to the weakened coherence effect. The superposition between an arbitrary NDD state and another one corresponds to the vanishing limit of the coherence and be totally free from the effect of disorder. Thus it has $\mathcal{C}(r_i, \mathbf{q}) = 0$ with $r_i \rightarrow \infty$ in this case, and this region is absent in the torus diagram of the phase space (Fig.6). In other word, $\mathcal{C}(r_i, \mathbf{q}) = 1$ and $\mathcal{C}(r_i, \mathbf{q}) = 0$ correspond to the presence and absence of global (disorder-induced) fluctuation, respectively. There are also fluctuations for nonintegrable case with $0 < \mathcal{C}(r_i, \mathbf{q}) < 1$, but it is due to the nonlocal symmetries with interaction, instead of due to the environmental disorder. In agree with our above result of Loschmidt echo, the integrability corresponding to large \mathbf{q} in phase space generates a Wigner distribution more easy to be reshaped (periodically [14]), as can be visualized by the boundary in the echo spectrum, under the effect of disorder (global fluctuation).

4.1 Berry conjecture in integrable side

Since the Berry's discussion mainly works on the integrable system where the correlations between the integrable eigenstates play a much important role than that between the nonintegrable eigenstates, we mainly focus on the integrable side in this section, which corresponds to the large fluctuation effect brought by the r_i within the above perturbations. Then in such case, the correlation between nonintegrable eigenstates can be ignored, i.e., the correlation effects between species ℓ_1 and ℓ_2 , thus we can temperately remove the subscripts from the two perturbations, and make them look different only from the integrable eigenstates fluctuation part. More specifically, such region where the integrability takes dominant role can be identified by the range where the inverse length of \mathbf{p} , i.e., the de Broglie wavelength, is larger than the characteristic length of r_i , within which range the Berry autocorrelation is close to one, and we will show below that this indeed, corresponds to the inverse participation ratio (IPR) which be finite (can be setted as one, as well) in the localized systems, in contrast to the systems with spatially extended states. While in the opposite side, where the de Broglie wavelength is very small (corresponds to the increased length of \mathbf{p}) and even smaller than the characteristic distance between V_1 and V_2 , the Berry autocorrelation becomes vaishingly small, in which case the distinct species of the nonintegrable eigenstates cannot be ignored anymore, and the system turns to the chaotic side.

In the integrable side, the selection of classical actions leads to the averaged results[4]

$$\begin{aligned} \overline{V(q + \frac{r_i}{2})V^*(q - \frac{r_i}{2})} &= \frac{\delta(E - \mathbf{p}^2 - \mathbf{q})}{\int d\mathbf{q} \int d\mathbf{p} \delta(E - \mathbf{p}^2 - \mathbf{q})}, \\ |\overline{V(q)}|^2 &= \frac{\int d\mathbf{p} \delta(E - \mathbf{p}^2 - \mathbf{q})}{\int d\mathbf{q} \int d\mathbf{p} \delta(E - \mathbf{p}^2 - \mathbf{q})} = \frac{(E - \mathbf{q})^\eta}{\int d\mathbf{q} (E - \mathbf{q})^\eta}, \end{aligned} \quad (5)$$

where $\eta = \frac{-1}{2}$ in the caustics point, and $\eta = 0$ in other points locate in the integrable region. As shown in Fig.6, in the systems where integrability is dominant, the length of \mathbf{p} is very small, which has very simple expression $|\mathbf{p}| = \sqrt{E - \mathbf{q}}$,

in aid of the selection of the actions through the n -dimensional delta function, where here n is the number of distinct good quantum numbers, which is also the number of local sites that participate in the average calculation here.

Specifically, near the caustic point, we have the following relation

$$\mathbf{p}^2 = \mathbf{q}[\mathbf{p}], \quad (6)$$

i.e., the squared \mathbf{p} can be replaced by the $\mathbf{q}[\mathbf{p}]$ as a functional of \mathbf{p} , and the caustic point satisfies

$$\mathbf{q}[\mathbf{p}] = \mathbf{q}[0] = \mathbf{q}, \quad (7)$$

which indicate the special property when near the caustic point of a torus, i.e., the large variance of $\frac{d\theta}{dq}$ in terms of the angle as shown in Fig.6. Also, we can know that E can be approximated as $2\mathbf{q}$ in this case.

Moreover, at the caustic point with $\eta = -1/2$, the numerator and denominator of the above local average function satisfies

$$\begin{aligned} \int d\mathbf{p} \delta(E - \mathbf{p}^2 - \mathbf{q}) &= \sum_i \mathbf{p}_i = \frac{1}{\mathbf{p}} = \frac{1}{\sqrt{\mathbf{q}[\mathbf{p}]}, \\ \int d\mathbf{q} \int d\mathbf{p} \delta(E - \mathbf{p}^2 - \mathbf{q}) &= \int d\mathbf{q} \mathbf{q}^{-1/2} = 1. \end{aligned} \quad (8)$$

We will mainly using this formula, which is for the ergodic system with stochastic classical motions and the influence of different \mathbf{p} on the functional $\mathbf{q}[\mathbf{p}]$ are uncorrelated, which make sure that the summation over the discrete samples \mathbf{p}_i are solely for a symmetry sector where each one are selected by the delta function.

Thus in this case the second moment of perturbation is

$$\overline{|V(q)|^2} = \frac{1}{\sqrt{\mathbf{q}[\mathbf{p}]}} = \frac{1}{\mathbf{p}}, \quad (9)$$

which turns to infinite due to the vanishing length of \mathbf{p} . In the above ergodic-type expressions for the averaged Wigner function, the selection of delta-function takes effect, but in the mean time the selection results in a special configuration that the local and nonlocal conservations coexist. This will be explained below section, in terms of the infinite series over the discrete samples selected (or filtered) by the delta functions that depending on the overlap (or classical analog) between the classical energy surface and the classical actions, where nonlocal conservations are perserved by the selections (in the same pattern) and form a certain symmetry sector. In the integrable system, such nonlocal conservation is dominant, in comparasion to the Gaussian randomness which is brought by the local conservation and related to the non-negligible effect of integrable eigenstate fluctuation.

5 Application of the method correlations of the adjacent local states (CALs)

Next we apply the method base on the estimation of the correlations of the adjacent local states (CALs), where the nearby local states form a continuum and conserved observation, whose nonlocal symmetry properties can be projected to the invariant microcanonical averages within the narrow microcanonical intervals formed by the scaled variables. Details about the CALs is presented in Supplemental Material.

When the system is in the integrable and nonergodic side, where the characteristic de Broglie wavelength is much larger than the integrable state's fluctuation, we use an analysis expression to represent the projection \mathbf{p} ,

$$\frac{1}{\mathbf{p}} = \lim_{k \rightarrow \infty} \sum_{\gamma=0}^{k-1} \left(\frac{1}{z}\right)^\gamma = \frac{z}{z-1}, \quad (10)$$

while the quantity \mathbf{q} can be expressed as

$$\frac{1}{\sqrt{\mathbf{q}}} = \frac{I_0}{f_0} = 1 - \frac{1}{\partial_{k+} f_0}. \quad (11)$$

Note that the method CALs used here requires the definition of the following quantities, where more details are presented in Appendix.A,

$$\begin{aligned} f_0 &= \frac{1}{\mathbf{p}}, \\ I_0 &= f_0 \frac{\partial_{k+} f_0 - 1}{\partial_{k+} f_0}. \end{aligned} \quad (12)$$

Equivalently, in terms of such discrete summations there is, according to the Berry conjecture, another equivalent expression for $\overline{|V(q)|^2}$ which is more nonergodic-type, but also scales to infinite in the caustic point just like the above expression[4],

$$\overline{|V(q)|^2} = \delta(\mathbf{I}(\mathbf{p}, \mathbf{q}) - \mathbf{I}_n), \quad (13)$$

where \mathbf{I}_n is the local average of the actions corresponding to the pathological nonergodic classical motions in the phase space, and each \mathbf{I}_n corresponds to a good quantum number that plays the role of the power of integrable state generator. Using the property of delta-function $\delta(f(x)) = \sum_i \frac{\delta(x-x_i)}{|\partial_x f(x)|}$, with x_i are roots of $f(x)$, we obtain

$$\overline{|V(q)|^2} = \frac{1}{\sqrt{\mathbf{q}}} = \frac{I_0}{f_0} = \sum_{ki} \left| \frac{d\mathbf{I}(\mathbf{q}, \mathbf{p}_{ki})}{d\mathbf{p}} \right|^{-1} = \sum_i \left| \frac{d\boldsymbol{\theta}(\mathbf{q}, \mathbf{p}_i)}{d\mathbf{q}} \right| = \frac{\partial_{k+} f_0 - 1}{\partial_{k+} f_0}, \quad (14)$$

where the differentials are related to the local quantities through

$$\begin{aligned} \left[\sum_i \left| \frac{d\boldsymbol{\theta}(\mathbf{q}, \mathbf{p}_{ki})}{d\mathbf{q}} \right| \right]^{-1} &= \sum_{\gamma=0}^{\infty} \left(\frac{1}{\partial_{k+} f_0} \right)^{\gamma}, \\ \sum_i \left| \frac{d\mathbf{I}(\mathbf{q}, \mathbf{p}_i)}{d\mathbf{p}} \right|^{-1} &= \sum_{i=1}^{\infty} \left(1 - \frac{f_0}{I_0} \right)^{i-1}, \end{aligned} \quad (15)$$

where we also have

$$\begin{aligned} \sum_i \left| \frac{d\boldsymbol{\theta}(\mathbf{q}, \mathbf{p}_i)}{d\mathbf{q}} \right| &= \left| \frac{d \sum_i \boldsymbol{\theta}(\mathbf{q}, \mathbf{p}_i)}{d\mathbf{q}} \right| = \frac{\partial_{k+} f_0 - 1}{\partial_{k+} f_0} = [\partial_k (I_0 - f_0)]^{-1}, \\ \sum_{ki} \left| \frac{d\mathbf{I}(\mathbf{q}, \mathbf{p}_{ki})}{d\mathbf{p}} \right| &= \sum_{i=1}^{\infty} \left(\frac{I_0}{I_0 - f_0} \right)^{i-1} = \sum_{i=1}^{\infty} (1 - \partial_{k+} f_0)^{i-1}, \end{aligned} \quad (16)$$

and through the sampling rule for the indices of \mathbf{p} in the summation, we can obtain

$$\begin{aligned} \frac{d\mathbf{I}(\mathbf{q}, \mathbf{p}_{ki})}{d\mathbf{p}} &= \partial_{k+} f_0, \\ \left| \frac{d\boldsymbol{\theta}(\mathbf{q}, \mathbf{p}_i)}{d\mathbf{q}} \right| &= \frac{f_0}{I_0} = \frac{\partial_{k+} f_0}{\partial_{k+} f_0 - 1}, \end{aligned} \quad (17)$$

where the first expression is deduced in Appendix.B. Here, for convenience of analytical analysis, we define $\frac{1}{\mathbf{p}} = \frac{z}{z-1}$ with z a positive real integer (for more details see Appendix.A). Here we use another infinite quantity in caustic point $\frac{1}{\sqrt{\mathbf{q}}}$ instead of $\frac{1}{\mathbf{p}}$, and in fact these two quantities has minor difference even in caustic point, as discussed in below section; While for the second expression, in comparasion with Eq.(16), we obtain

$$\frac{d \sum_i \boldsymbol{\theta}(\mathbf{q}, \mathbf{p}_i)}{d \boldsymbol{\theta}(\mathbf{q}, \mathbf{p}_i)} = \frac{I_0^2}{f_0^2} = [\partial_k (I_0 - f_0)]^{-2} = I_0 \partial_{k+} \frac{I_0}{f_0}. \quad (18)$$

In the first line of Eq.(8) the selection of delta function results in the summation over the local sites labeled by i , and we have the following expressions,

$$\sum_i \mathbf{p}_i = \sum_i \mathbf{p}_i[\mathbf{q}] = \sum_{i=1}^{\infty} (1-p)^{i-1} = \sum_{i=1}^{\infty} \left(\frac{1}{z} \right)^{i-1} = \frac{z}{z-1} = \frac{1}{\mathbf{p}}. \quad (19)$$

Then in the integrable side, the averaged Wigner function in the first line of Eq.(5) can be rewritten as

$$\overline{V(q + \frac{r_i}{2}) V^*(q - \frac{r_i}{2})} = \delta(E - \mathbf{p}^2 - \mathbf{q}) = \partial_i \left[\frac{1}{\mathbf{p}} \right]_i \approx \partial_{k+} \mathbf{I}[\mathbf{p} + k^+], \quad (20)$$

which corresponds to the maximal derivative of the classical action $\mathbf{I}[\mathbf{p} + k^+]$ on k^+ . Here we built a correspondence between the delta-function representation and the functional expansion of the classical action (which is the $\frac{1}{\mathbf{p}}$ here), where we present the details in Appendix.A, Appendix.B, and the Supplemental material. As we shown in Appendix.A, as the $\frac{1}{\mathbf{p}}$ increase to an largest extend, and nearly reaches the upper boundary of the k^+ -independent segment, which is represented by the functional $\mathbf{I}[\mathbf{p}]$, its dependence on k^+ is vanishingly small, in which occasion we can expand the k^+ -dependence of $\frac{1}{\mathbf{p}}$ in terms of the derivatives of the delta-type function in a series of order (as we shown in Appendix.A) and such correspondence is being further verified in terms of the second set of CALS as we shown in Sec.C in Supplemental material, where the dominant nonlocal effect smoothing the difference (and independence) between different segments. Then, in terms of teh method of CALS, the result in the second line of Eq.(8) can be rewritten as

$$\int d\mathbf{q} \int d\mathbf{p} \delta(E - \mathbf{p}^2 - \mathbf{q}) = \sum_i \left[\frac{I_0}{f_0} \right]_i = 1, \quad (21)$$

where the summation is over the discrete local points that are selected according to the rule of minimal local-variable-dependence, which is, inother word, maximal nonlocal chanracter. This can also be verified using the fnctional derivatives of the classical action with their corresponding variable as shown in Appendix.B

Importantly, here the classical analog between f_0 and $\frac{1}{\sqrt{\mathbf{q}}} = \frac{I_0}{f_0}$ originates from the their same derivatives with respect to k , which is the variable in one of the local points. In this perspective, we can further define the f_0 in terms

of an identity whose functional summation (which is indeed the integral containing selections by the delta function) is equivalent to taking the limit on the variable k^+ (with smaller variation than k), and in the mean time, remove the k^+ -dependence on f_0 through the homogenization on the averaged Wigner function with the local averaged one,

$$1_{k^+} = \delta(\partial_k \frac{I_0}{f_0}) = \sum_{p_0} e^{-ip_0 r_{i_0}} \overline{\sum_{i_0} e^{ip_0 r_{i_0}} \left[\frac{1}{N} \left(w_i \left(\frac{r_{i_0}}{2} \right) F[k^+] + w_i \left(-\frac{r_{i_0}}{2} \right) (1 - F[k^+]) \right) \right]}, \quad (22)$$

where p_0 , i_0 denote the projection and integrable state fluctuation in this subsystem, and w_i is the weight which leads to the finite k^+ -dependence on the identity 1_{k^+} . $F[k^+]$ is an arbitrary functional of k^+ . Note that in terms of a number one with finite k^+ -dependence, it all refers to the $\frac{1}{\mathbf{p}}$, until we using the notation $\frac{I_0}{f_0}$ which refers to the $\frac{1}{\sqrt{\mathbf{q}}}$, and the delta function of $\partial_k \frac{I_0}{f_0}$ in second term of above expression is only to indicate such common k -independent feature which is shared by both the $\frac{1}{\mathbf{p}}$ and $\frac{1}{\sqrt{\mathbf{q}}}$. The homogenization process is equivalent to making the Berry autocorrelation be one in this subsystem, i.e.,

$$\begin{aligned} \sum_{i_1} [1_{k^+}]_{i_1} &= \sum_{p_0} e^{-ip_0 r_{i_0}} \overline{\sum_{i_0} e^{ip_0 r_{i_0}} \left[\frac{1}{N} \left(w_i \left(\frac{r_{i_0}}{2} \right) F[k^+] + w_i \left(-\frac{r_{i_0}}{2} \right) (1 - F[k^+]) \right) \right]} \\ &\approx \sum_{p_0} \sum_{i_0} e^{ip_0 r_{i_0}} \left[\frac{1}{N} \left(w_i \left(\frac{r_{i_0}}{2} \right) F[k^+] + w_i \left(-\frac{r_{i_0}}{2} \right) (1 - F[k^+]) \right) \right] \\ &= \left[\sum_i \frac{1}{N} \left(w_i(0) F[k^+] + w_i(0) (1 - F[k^+]) \right) \right] = 1, \end{aligned} \quad (23)$$

where the summation over p_0 on the term with bottom line, i.e.,

$$\overline{\sum_{p_0} \sum_{i_0} e^{ip_0 r_{i_0}} \left[\frac{1}{N} \left(w_i \left(\frac{r_{i_0}}{2} \right) F[k^+] + w_i \left(-\frac{r_{i_0}}{2} \right) (1 - F[k^+]) \right) \right]}, \quad (24)$$

can be viewed as a local average over the k^+ -dependent region, similar to the classical action $\mathbf{I}[\mathbf{p} + k^+]$ in Eq.(43), and as system closes to the integrable side, which means the above local averaged term becomes very large and the summation turns to the selective one over the discrete terms following the same pattern (see Eq.(45)), and in the mean time, the derivative of such local averaged term becomes vanishingly small, and the nonlocal correlations between the adjacent regions (or segments) become overwhelming that the local correlations inside the single segment. Thus the p_0 (within the term $e^{-ip_0 r_{i_0}}$) is, quite reasonably, vanishingly small due to the selection effect, and now the above averaged Wigner function becomes the same with the local average density function, where the effect of r_{i_0} has been smoothed out by the average. Here the summation over i_1 corresponds to taking the limit $k^+ \rightarrow \infty$. Note that the result in Eq.(23), which is one, indeed does not directly reflect the quantitative value of the local averaged function itself, but in terms of the variable of the next segment k^+ , as a result of the large fluctuation in the boundaries, which leads to more nonlocal correlation, and less locally distinctive features (see Appendix.A for an example). We also note that, what we mean by large integrable eigenstate fluctuation here, counterintuitively, corresponds to less effect from the boundary exchanging term r_{i_0} , after the average in the last line of Eq.(23). This is because the r_{i_0} term here does not represent the oscillator amplitude which is inversely proportional to the number of local oscillators (and thus also to the nonlocal correlation). While here the large fluctuation of boundary exchanging term r_{i_0} is related to the low dimensional condition as shown in Eq.(5) where $\eta = -1/2 = \frac{d}{2} - 1$ corresponds to the effective dimension $d = 1$ here, and the large fluctuation leads to smaller variance as well as the enhanced homogenization between the adjacent segments, where the individual characteristics of different segments fade to some extent.

Now we have the smoothed version of $1_{k^+} (= \frac{1}{\mathbf{p}})$, which we express it using z' ,

$$\sum_{i_1} [1]_{i_1} = \frac{z'}{z' - 1} \sum_{i_2} \left[1 - \left(\frac{1}{z'} \right)^{k^+} \right]_{i_2} = \frac{z'}{z' - 1}, \quad (25)$$

and thus $f_0 = \sum_{\gamma=0}^{k^+-1} \left(\frac{1}{z'} \right)^\gamma$. Here the summation over i_2 represents taking the limit $k^+ \rightarrow \infty$ for the part within the bracket, which is indeed the fluctuation from the lower boundary of the upper segment into the current k^+ -dependent segment. The identity embedded in the above expression satisfies

$$\sum_{i_2} \left[1 - \left(\frac{1}{z'} \right)^{k^+} \right]_{i_2} = 1. \quad (26)$$

This is a very important result, and we will explain it latter.

Note that $z' \neq z$, otherwise $\lim_{k^+ \rightarrow \infty} f_0 = f_0$. Also, we have the expression

$$\lim_{k^+ \rightarrow \infty} f_0 = \lim_{k^+ \rightarrow \infty} \left(\lim_{k \rightarrow \infty} f_1 \right) = \frac{f_0}{1 - \left(\frac{1}{z'} \right)^{k^+}} = \frac{z'}{z' - 1}, \quad (27)$$

where the derivative of f_0 with respect to k^+ is $\partial_k f_0 = \frac{(\partial_k f_1)^2}{\partial_k f_1 - 1}$ (see Appendix.A). $f_1 = \sum_{\gamma=0}^{k-1} \left(\frac{1}{z}\right)^\gamma$ is the generator of f_0 , and we can obtain f_0 by smooth out the k -dependence on f_1 , $f_0 = \lim_{k \rightarrow \infty} f_1$.

Thus more precisely, the difference between $\frac{1}{\mathbf{p}}$ and $\frac{1}{\sqrt{\mathbf{q}}}$ is that they identify the upper boundary and lower boundary of the region where can be estimated as that the k -dependence has being smoothed out, that is to say,

$$\partial_{k^+} \frac{1}{\mathbf{p}} \neq 0, \quad \partial_{k^+} \left(\frac{1}{\mathbf{p}} + 0^+\right) = 0, \quad \partial_k \frac{1}{\sqrt{\mathbf{q}}} = 0, \quad \partial_k \left(\frac{1}{\sqrt{\mathbf{q}}} - 0^-\right) \neq 0. \quad (28)$$

Thus to make sure $\frac{1}{\mathbf{p}}$ and $\frac{1}{\sqrt{\mathbf{q}}}$ are locate in the correct boundaries of the k -independent region, we make an important assumption for the terms in Eq.(26), i.e.,

$$\left(\frac{1}{z'}\right)^{k^+} = \frac{1}{\partial_{k^{++}}(I_0 - f_0)} = \partial_{k^+} f_0 = 0, \quad (29)$$

where we use the formula presented in Appendix.A, $\partial_{k^{++}}(I_0 - f_0) = \frac{1}{\partial_{k^+} f_0}$, thus the approximation at the boundary $\partial_{k^+} f_0 \approx 0$ is equivalents to the $\partial_{k^{++}}(I_0 - f_0) = \infty$. The above equality guarantees we can correctly identify the lower boundary of the k^{++} -independent segment which is the $\frac{I_{02}}{f_{02}}$ (see Appendix.A). In the mean time, as we discuss in Appendix.A, when we set $\partial_{k^+} f_0 = \left(\frac{1}{z'}\right)^{k^+}$ is nearly zero, the corresponding k^+ -dependent term $(1 - \left(\frac{1}{z'}\right)^{k^+})$ now indeed represent the largest possible fluctuation of the lower boundary of k^+ -independent segment $\left(\frac{I_{02}}{f_{02}}\right)$ into the k -independent segment, and the summation over i_2 remove such fluctuation-induced k -dependence. When such k -dependence of the lower boundary of upper segment is completely removed (after the local average on a certain boundary), the random fluctuations play no role and the perturbations are deviated from random Gaussian function, and the Wigner average reduces to the local average and results in the Berry anticorrelation \mathcal{C} be nearly one, which also corresponds to the maximized IPR (corresponds to the many-body localization phase). Note that for arbitrarily two adjacent segments, the fluctuations of the lower boundary of upper segment and that of the upper boundary of the lower segment are mutually correlated, just like the integrable eigenstate fluctuations represented by $\pm \frac{r_i}{2}$ in Eq.(2).

Also, we note that $\frac{I_{02}}{f_{02}}$ is related to the lower boundary of the k -independent segment by $\frac{I_{02}}{f_{02}} = \lim_{k^+ \rightarrow \infty} \frac{1}{\sqrt{\mathbf{q}}} = \lim_{k^+ \rightarrow \infty} \frac{I_0}{f_0}$.

The summation over i_2 reads

$$\sum_{i_2} \left[1 - \left(\frac{1}{z'}\right)^{k^+}\right]_{i_2} = \sum_{i_2} [1 - O(\partial_{k^+} f_0 + 0^+)]_{i_2} = \sum_{i_2} [1]_{i_2} = \frac{I_{02}}{f_{02}}, \quad (30)$$

where the $[1]_{i_2}$ here is the lower boundary of the k^+ -independent segment but being endowed the maximal k^+ -dependence through the fluctuation. Assuming such largest fluctuation is possible to reaches the bottom of the lower segment (see Appendix.A), then $\frac{I_{02}}{f_{02}}$ should shares the feature of $\frac{I_0}{f_0}$, and the summation over i_2 is then similar to Eq.(22,23).

Following the same pattern due to the nonlocal symmetry, for k^- -independent segment, which is below the k -independent one, the quantity in bottom of k^- -independent segment reads

$$1_k = \delta\left(\partial_k - \frac{I_{01}}{f_{01}}\right) = \sum_{p_{01}} e^{-ip_{01}r_{i_{01}}} \overline{\sum_{i_{01}} e^{ip_{01}r_{i_{01}}} \left[\frac{1}{N}(w_i\left(\frac{r_{i_{01}}}{2}\right)F[k] + w_i\left(-\frac{r_{i_{01}}}{2}\right)(1 - F[k]))\right]}, \quad (31)$$

where $r_{i_{01}}$ represents the the smoothing process for the k -dependence can be expressed as

$$\begin{aligned} \sum_{i_1} [1]_{i_1} &\approx \sum_{p_{01}} \sum_{i, i_{01}} e^{ip_{01}r_{i_{01}}} \left[\frac{1}{N}(w_i\left(\frac{r_{i_{01}}}{2}\right)F[k] + w_i\left(-\frac{r_{i_{01}}}{2}\right)(1 - F[k]))\right] \\ &= \overline{\left[\sum_i \frac{1}{N}(w_i(0)F[k] + w_i(0)(1 - F[k]))\right]} = \frac{I_{01} - f_{01}}{\frac{I_{01}}{f_{01}}} \\ &= \frac{f_{01}}{1 - \partial_k f_{01}} \sum_{i_3} [1 - \partial_k f_{01}]_{i_3} = \frac{f_{01}}{1 - \partial_k f_{01}} = \frac{I_0}{f_0}, \end{aligned} \quad (32)$$

where

$$\begin{aligned} I_{01} - f_{01} &= \frac{-f_{01}}{\partial_k f_{01}}, \\ \frac{I_{01}}{f_{01}} &= \frac{\partial_k f_{01} - 1}{\partial_k f_{01}}, \end{aligned} \quad (33)$$

and, still, the summation over i_3 correspond to smoothing of the k^- -dependence, where $\sum_{i_3} [1]_{i_3} = \frac{I_{01}}{f_{01}}$ is the lower boundary of the k^- -independent region, with $\partial_k(f_{01} + 0^+) = 0$.

6 Conclusion

We propose a method to constructing the commensurate eigenvector basis that are appropriate for the numerical calculation as well as the diagonal or off-diagonal ETH diagnostics. We also investigate the integrability-chaos transition with independent perturbations in terms of the Berry autocorrelation in semiclassical limit, where there is a phase space spanned by the momentum-like projection and the range of local wave function. We also develop a method, CALS, to investigate the integrability-chaos transition. In the presence of uncorrelated perturbations and correlated integrable eigenstate fluctuations, which is applicable for both the ergodic and nonergodic systems. More importantly, this work reveals and illustrates to a certain extent the essential role of the Golden ratio and the constant $\frac{1}{3}$ in the quantum chaos physics.

7 Appendix.A: Proof of Eq.(30) using the first set of CALS

For each segment with a certain $\{k\}$ -dependent, using the above formulas, the limiting results for the upper and lower boundaries are just the upper and lower boundaries of the segment above it which has a dependence on larger $\{k\}$. For each segment, the upper boundary is the (like the $\frac{1}{\mathbf{p}}$ in the k^+ -dependent region) is infinitely close to the lower boundary of the above segment (like the $\frac{1}{\sqrt{q}} = \frac{I_{02}}{f_{02}} = 1_{k^{++}}$ in Fig.), also, in terms of the first set of CALS connecting the present segment and the above segment, the lower boundary of the above segment plays the role of unit quantity in the denominator of the limiting expression. To illustrate this, we firstly consider the two sets of CALS which connecting the segment be independent of k and the segment be independent of k^+ ,

$$\lim_{k^+ \rightarrow \infty} \frac{1}{\mathbf{p}} = \frac{z'}{z' - 1} \lim_{k^+ \rightarrow \infty} f_0 = \frac{f_0}{1_{k^{++}} - \partial_{k^+} f_0}, \quad (34)$$

where

$$\begin{aligned} \frac{1}{\mathbf{p}} &= f_0 = \lim_{k \rightarrow \infty} f_1 = \frac{z}{z - 1} = \sum_{\gamma=0}^{k^+-1} \left(\frac{1}{z'}\right)^\gamma, \\ f_1 &= \sum_{\gamma=0}^{k^+-1} \left(\frac{1}{z}\right)^\gamma \end{aligned} \quad (35)$$

with z' determined by the

$$\frac{1}{z'} = \left[\frac{(\partial_k f_1)^2}{\partial_k f_1 - 1} \right]^{1/k^+}, \quad (36)$$

which can be obtained from formula Eq.(S18) in the Supplemental material.

Then there is a singularity when we try to check the derivative $\partial_{k^+} f_0$ in terms of the formula eq.(34), that is,

$$\partial_{k^+} \left[\left(\lim_{k^+ \rightarrow \infty} \frac{1}{\mathbf{p}} \right) (1_{k^{++}} - \partial_{k^+} f_0) \right] \neq \partial_{k^+} f_0, \quad (37)$$

this is inevitable due to the finite overlaps appear in the two boundaries (where $\partial_{k^+}(\frac{1}{\mathbf{p}} + 0^+) = 0$, and $\partial_k(\frac{1}{\sqrt{q}} - 0^+) \neq 0$), however, we can make an approximation where $k^+ \rightarrow \infty$, then we have

$$\partial_{k^+}^{(2)} f_0 = \frac{1 - \partial_{k^+} f_0 + (\partial_{k^+} f_0)^2 - (\partial_{k^+} f_0)^3}{(\partial_{k^+} f_0) f_0} \quad (38)$$

which is close to the actual result (using the formulas Eqs.(S15-S18) in supplemental material)

$$\partial_{k^+}^{(2)} f_0 = \partial_{k^+} \frac{f_0^2}{I_0(f_0 - I_0)} = \frac{(\partial_{k^+} f_0)^2 [2 + 3\partial_{k^+} f_0 - 2(\partial_{k^+} f_0)^2 - 2(\partial_{k^+} f_0)^3 + (\partial_{k^+} f_0)^4]}{(-1 + \partial_{k^+} f_0) f_0} \quad (39)$$

in the limit of $\partial_{k^+} f_0 = 0$. This result is consistent with that obtained using the delta-function representation as shown in Appendix.B (Eq.(45)), where $\partial_{k^+} f_0 = \frac{1}{k^+!} \delta^{(k^+)}(k^+) \varepsilon^{k^+}$, and using this result we got

$$\partial_{k^+}^{(2)} f_0 = \left(\frac{\varepsilon^k (k! \log(\varepsilon) - \Gamma(k+1) \Psi^{(0)}(k+1))}{(k!)^2} \right) \delta^{(k^+)}(k^+) + \frac{\varepsilon^{k^+}}{k^+!} \delta^{(k^++1)}(k^+) = 0, \quad (40)$$

where Ψ is the polygamma function $\Psi^{(0)}(k^+ + 1) = \Psi^{(0)}(k^+) + \frac{1}{k^+}$. In this approximation, we assume $1_{k^{++}}$ (i.e., $\mathbf{I}[\mathbf{p}]$ in the Appendix.B) is being endowed with the maximal k^+ -dependence which corresponds to the lower boundary of the k^+ -dependent segment, i.e., $\frac{I_{02}}{f_{02}} \rightarrow \frac{I_0}{f_0}$, and

$$\partial_{k^+} \frac{I_{02}}{f_{02}} = \partial_{k^+} \frac{I_0}{f_0} = \frac{I_0}{f_0^2} = \frac{\partial_{k^+} f_0 - 1}{f_0 \partial_{k^+} f_0}, \quad (41)$$

Then combining Eqs.(38,41), the Eq.(37) becomes

$$\left(\lim_{k^+ \rightarrow \infty} \frac{1}{\mathbf{p}} \right) \partial_{k^+} [(1_{k^{++}} - \partial_{k^+} f_0)] = \partial_{k^+} f_0. \quad (42)$$

This corresponds to a hypothesis in the extreme case where $\frac{I_{02}}{f_{02}}$ reaches its minimal value (even much larger than $\partial_{k^+} f_0$ since f_0 is vanishingly small now) due to the fluctuation and $\partial_{k^+} \frac{I_{02}}{f_{02}}$ reaches the maximal value. In the mean time, since now there without the k^+ -independent part (all be overlapped by the k^+ -independent segment), the f_0 should nearly equals to zero, in terms of the delta-function correspondence as shown in Appendix.B.

8 Appendix.B: Functional form of $\frac{1}{\mathbf{p}}$ and the classical action (Proof of Eq.(17))

In terms of the functional definition for the classical actions, there is another expression for the $\frac{1}{\mathbf{p}}$, which is consistent with Eq.(25). The $\frac{1}{\mathbf{p}}$ can also reads

$$\mathbf{I}[p + k^+] = \mathbf{I}[p] + \sum_{n=1}^{\infty} \frac{1}{n!} \frac{d^{(n)} \mathbf{I}[p + k^+]}{d\varepsilon^{(n)}} \Big|_{\varepsilon=0} \varepsilon^n, \quad (43)$$

where \mathbf{p} plays the role of function, and $k^+ = \varepsilon \eta$ is the variation of it. $\mathbf{I}[p]$ represent the lower boundary of the k^+ -independent region, i.e., $\mathbf{I}[p]$ is equivalent to $(\frac{1}{\mathbf{p}} + 0^+)$ (see second line of Eq.(28)),

$$\begin{aligned} \mathbf{I}[p] &= 1_{k^{++}} = \frac{I_{02}}{f_{02}}, \\ f_{02} &= \frac{z_2}{z_2 - 1}, \\ I_{02} &= f_{02} \frac{\partial_{k^{++}} f_{02} - 1}{\partial_{k^{++}} f_{02}}, \end{aligned} \quad (44)$$

where $\frac{z_2}{z_2 - 1}$ is, follow the above routine, the upper boundary in the k^+ -independent region. Thus $\mathbf{I}[p]$ can be simply written as $1 (= \frac{d^{(0)} \mathbf{I}[p + k^+]}{d\varepsilon^{(0)}} \Big|_{\varepsilon=0} \varepsilon^0)$ in the first term of expanded functional $\mathbf{I}[p + k^+]$.

Next we show how to related such functional definition to the series definition given in Eq.(25). This requires viewing the n -th order functional derivatives of the functional $\mathbf{I}[\mathbf{p} + k^+]$ as the n -th derivatives of delta function, then we have the following correspondence (for $n \leq k^+ - 1$),

$$\begin{aligned} \frac{1}{z'} &= \frac{d\mathbf{I}[p + k^+]}{d\varepsilon} \Big|_{\varepsilon=0} \varepsilon = \delta^{(1)}(k^+) \varepsilon, \\ \dots \\ \left(\frac{1}{z'} \right)^n &= \frac{1}{n!} \frac{d^{(n)} \mathbf{I}[p + k^+]}{d\varepsilon^{(n)}} \Big|_{\varepsilon=0} \varepsilon^n = \frac{1}{n!} \delta^{(n)}(k^+) \varepsilon^n, \end{aligned} \quad (45)$$

then we use the property of delta function $\frac{\delta^{(n)}(x)}{\delta(x)} = \frac{(-1)^n n!}{x^n}$, and obtain

$$(\delta^{(1)}(k^+) \varepsilon)^n = (-\frac{1}{k^+} \delta(k^+) \varepsilon)^n = \frac{1}{n!} \delta^{(n)}(k^+) \varepsilon^n = \frac{1}{n!} \delta(k^+) \frac{(-1)^n n!}{(k^+)^n} \varepsilon^n. \quad (46)$$

Then the *varepsilon* indeed represent the variation of k^+ ($\varepsilon \sim 1/k^+$), and in the limit of $k^+ \rightarrow \infty$, f_0 (in terms of the delta-function representation) reduced to $\mathbf{I}[\mathbf{p}] = 1_{k^{++}}$, which is the lower boundary of the above segment. Since here the $\mathbf{I}[\mathbf{p} + k^+]$ (or $\frac{1}{\mathbf{p}}$) is the lower boundary of the k^+ -dependent region, we use the delta function of the first order derivative to represent the most notable part of the remaining k^+ -dependence, and thus we donot have to pay attention to the terms with higher power, i.e., we use $\delta(k^+) = \delta^a(k^+)$ for $a > 1$.

The differential of $\mathbf{I}[\mathbf{p} + k^+]$ reads

$$\begin{aligned} \frac{d\mathbf{I}[\mathbf{p} + k^+]}{d\varepsilon} &= \sum_{n=1}^{\infty} \frac{d^{(n)} \mathbf{I}[\mathbf{p} + k^+]}{d\varepsilon^{(n)}} \Big|_{\varepsilon=0} \frac{\varepsilon^{n-1}}{(n-1)!} \\ &= \sum_{n=1}^{\infty} \int dx_1 \cdots dx_n \frac{\delta^{(n)} \mathbf{I}[\mathbf{p}]}{\delta \mathbf{p}(x_1) \cdots \delta \mathbf{p}(x_n)} \eta(x_1) \cdots \eta(x_n) \frac{\varepsilon^{n-1}}{(n-1)!}, \end{aligned} \quad (47)$$

to exhibit the main effect in the first term on the functional expansion, we assume there is exists a series of certain discrete coordinates x which satisfy

$$\frac{d\mathbf{I}[\mathbf{p} + k^+]}{d\varepsilon} = \sum_x \frac{\delta \mathbf{I}[\mathbf{p}]}{\delta \mathbf{p}(x)} \eta(x), \quad (48)$$

then we have

$$d\mathbf{I}[\mathbf{p}] = \sum_x \left[\frac{\partial \mathbf{I}[\mathbf{p} + k^+]}{\partial \mathbf{I}[\mathbf{p}]} \right]^{-1} \frac{\partial \mathbf{I}[\mathbf{p}]}{\partial \mathbf{p}(x)} d(\eta(x)\varepsilon) = \sum_x \frac{\partial \mathbf{I}[\mathbf{p}]}{\partial \mathbf{p}(x)} d(\mathbf{p}(x)), \quad (49)$$

where the average over x satisfies

$$\overline{\left[\frac{\partial \mathbf{I}[\mathbf{p} + k^+]}{\partial \mathbf{I}[\mathbf{p}]} \right]^{-1}} d(\eta(x)\varepsilon) = d(\mathbf{p}(x)), \quad (50)$$

$$\overline{\frac{\partial \mathbf{p}(x)}{\partial(\eta(x)\varepsilon)}} = \frac{\partial \mathbf{I}[\mathbf{p}]}{\partial \mathbf{I}[\mathbf{p} + k^+]} \approx 1,$$

then since $d(\mathbf{p}(x))$ in the right-hand-side of Eq.(49) is an averaged result over the discrete coordinates x , we can move it to the left-hand-side, and then we obtain the Eq.(17). The reason why the set of coordinates satisfying Eq.(48) has the averaging behavior shown above, is that the coordinates which have $\overline{\frac{\partial \mathbf{p}(x)}{\partial(\eta(x)\varepsilon)}} = 1$ must be those where \mathbf{p} is (at least locally) in a minimal length, (and thus a minimal $\frac{\partial \mathbf{I}[\mathbf{p}]}{\partial \mathbf{p}}$, which inversely proportional to the fluctuation of the integrable eigenstate in this subsystem),

$$\overline{\frac{\partial \mathbf{I}[\mathbf{p} + k^+]}{\partial(\eta(x)\varepsilon)}} = \overline{\frac{\partial \mathbf{I}[\mathbf{p}]}{\partial \mathbf{p}(x)}} \rightarrow 0, \quad (51)$$

Thus the term $\frac{\delta \mathbf{I}[\mathbf{p}]}{\delta \mathbf{p}(x)} \eta(x)$ in Eq.(48) of each position x representing a local average for the $\frac{d\mathbf{I}[\mathbf{p} + k^+]}{d\varepsilon}$. As the system turns to the integrable region and close to the caustic point, the averaged Wigner function tends the same form with local averaged density function and thus the role of fluctuation can be smoothed out after the average which reflects the lowered randomness and higher pathologically distribution. Also, this is the case where all the functional derivative terms in Eq.(43) are independent with both $\mathbf{I}[\mathbf{p}]$ and $\mathbf{I}[\mathbf{p} + k^+]$.

References

- [1] Yurovsky, Vladimir A. "Exploring integrability-chaos transition with a sequence of independent perturbations." *Physical Review Letters* 130.2 (2023): 020404.
- [2] Shiraishi, Naoto, and Takashi Mori. "Systematic construction of counterexamples to the eigenstate thermalization hypothesis." *Physical review letters* 119.3 (2017): 030601.
- [3] Lyu, Chenguang Y., and Wen-Ge Wang. "A Physical Measure for Characterizing Crossover from Integrable to Chaotic Quantum Systems." *Entropy* 25.2 (2023): 366.
- [4] Berry, Michael V. "Regular and irregular semiclassical wavefunctions." *Journal of Physics A: Mathematical and General* 10.12 (1977): 2083.
- [5] Berkooz, Micha, et al. "Comments on the random Thirring model." *Journal of High Energy Physics* 2017.9 (2017): 1-27.
- [6] Bi, Zhen, et al. "Instability of the non-Fermi-liquid state of the Sachdev-Ye-Kitaev model." *Physical Review B* 95.20 (2017): 205105.
- [7] Shiraishi, Naoto, and Takashi Mori. "Systematic construction of counterexamples to the eigenstate thermalization hypothesis." *Physical review letters* 119.3 (2017): 030601.
- [8] Cao, Zan, Zhenyu Xu, and Adolfo del Campo. "Probing quantum chaos in multipartite systems." *Physical Review Research* 4.3 (2022): 033093.
- [9] Khasseh, Reyhaneh, et al. "Many-body synchronization in a classical hamiltonian system." *Physical review letters* 123.18 (2019): 184301.
- [10] You, Yi-Zhuang, Andreas WW Ludwig, and Cenke Xu. "Sachdev-Ye-Kitaev model and thermalization on the boundary of many-body localized fermionic symmetry-protected topological states." *Physical Review B* 95.11 (2017): 115150.
- [11] Mondaini, Rubem, et al. "Comment on "systematic construction of counterexamples to the eigenstate thermalization hypothesis"." *Physical review letters* 121.3 (2018): 038901.
- [12] Shiraishi, Naoto, and Takashi Mori. "Systematic construction of counterexamples to the eigenstate thermalization hypothesis." *Physical review letters* 119.3 (2017): 030601.
- [13] Chen-Huan Wu. "Statistic behaviors of gauge-invariance-dominated 1D chiral current random model." *Physica Scripta* (2022). <https://doi.org/10.1088/1402-4896/acdccc>.
- [14] Yurovsky, Vladimir A. "Exploring integrability-chaos transition with a sequence of independent perturbations." *Physical Review Letters* 130.2 (2023): 020404.
- [15] Medenjak, Marko, Tomaž Prosen, and Lenart Zadnik. "Rigorous bounds on dynamical response functions and time-translation symmetry breaking." *SciPost Physics* 9.1 (2020): 003.
- [16] Beugeling, Wouter, Roderich Moessner, and Masudul Haque. "Off-diagonal matrix elements of local operators in many-body quantum systems." *Physical Review E* 91.1 (2015): 012144.

- [17] Peacock, J. Clayton, and Dries Sels. "Many-body delocalization from embedded thermal inclusion." *Physical Review B* 108.2 (2023): L020201.
- [18] Anza, Fabio, Christian Gogolin, and Marcus Huber. "Eigenstate thermalization for degenerate observables." *Physical Review Letters* 120.15 (2018): 150603.
- [19] Cheng, Jun-Qing, Shuai Yin, and Dao-Xin Yao. "Dynamical localization transition in the non-Hermitian lattice gauge theory." *Communications Physics* 7.1 (2024): 58.
- [20] Cecile, Guillaume, Jacopo De Nardis, and Enej Ilievski. "Squeezed ensembles and anomalous dynamic roughening in interacting integrable chains." *Physical Review Letters* 132.13 (2024): 130401.

Supplemental Materials: Correlations of adjacent local states (CALs)

For eigenvalues arranged in ascending order in the target space, in terms of the effective (conditiona) entropy, the effective degrees of freedom and the mutual information can be measured and can be proved that follows the ensemble-dominated behaviors.

A First set of CALs: minimal (IR) cutoff-dependent CALs

We start by introducing two sets of quantities. For discrete summation described by $f_0 := \sum_{\gamma}^{k-1} \frac{1}{z^{\gamma}}$, with z a complex argument, we express its infinitely scaled form as

$$\lim_{k \rightarrow \infty} f_0 = \frac{f_0}{1 - \partial_k f_0}, \quad (\text{S1})$$

where $\partial_k f_0 = \frac{1}{z^k}$ and the dependence on background variable k is vanished in terms of this scaled form, which leads to the relation

$$\frac{\partial_k f_0}{f_0} = \partial_k \ln(1 - \partial_k f_0), \quad (\text{S2})$$

where the right-hand-side equals to $\partial_k \ln(\partial_k f_0 - 1)$ since $\ln(-1) = 0$ here which is guaranteed by the finite IR cutoff in terms of the fix step length during the derivation. This infinitely scaled result can be reexpressed as

$$\lim_{k \rightarrow \infty} f_0 = f_0 - \frac{f_0^2}{I_0}, \quad (\text{S3})$$

where $I_0 = f_0 \frac{\partial_k f_0 - 1}{\partial_k f_0}$. Now we have

$$\begin{aligned} \frac{I_0}{f_0} &= \frac{\partial_k f_0 - 1}{\partial_k f_0}, \\ \partial_k I_0 &= \partial_k f_0 - \frac{1}{\partial_k f_0}, \\ \partial_k \ln \frac{f_0}{I_0} &= \partial_k f_0 \left(\frac{I_0}{f_0^2} - \frac{1}{f_0} \right). \end{aligned} \quad (\text{S4})$$

By considering the scaled form of function $h_0 := (I_0 - f_0) = f_0 \frac{-1}{\partial_k f_0}$,

$$\lim_{k^- \rightarrow \infty} h_0 = I_0 = \frac{h_0}{1 - \partial_k h_0} = \frac{I_0 - f_0}{1 - \frac{f_0}{I_0}}, \quad (\text{S5})$$

$$\lim_{k \rightarrow \infty} h_0 = \frac{I_0 - f_0}{2f_0 - I_0} f_0 = \frac{h_0}{1 - \partial_k h_0} = \frac{I_0 - f_0}{1 - \frac{I_0 - f_0}{f_0}}. \quad (\text{S6})$$

Another scaling result with $k^+ \rightarrow \infty$, is

$$\lim_{k^+ \rightarrow \infty} h_0 = f_0 - \frac{f_0^2}{I_0} = \frac{h_0}{1 - \partial_k h_0} = \frac{I_0 - f_0}{1 - \frac{f_0 - I_0}{f_0}}. \quad (\text{S7})$$

As show in these two scaled results, we can see that there are different boundaries of infinity seted by different variables. The reason why $\partial_k h_0 \neq \frac{f_0}{I_0} = \frac{\partial_k f_0}{\partial_k f_0 - 1}$ is that for derivative with k the step length with expression of h_0 is indeed stretched in the above scaling form. That results in the distance-dependence during the derivation for two quantities that add or subtract. While for the first formula (Eq.(S5)), its derivative with respect to k^-

$$\partial_{k^-} h_0 = \frac{f_0}{I_0} = \frac{\partial_k f_0}{\partial_k f_0 - 1}, \quad (\text{S8})$$

is also related the result of $\partial_{k^+} \lim_{k \rightarrow \infty} f_0$: $\partial_{k^-} h_0 = \frac{\partial_{k^+} \lim_{k \rightarrow \infty} f_0}{\partial_k f_0}$.

When consider the derivative on Eq.(S1), as we discussed in Appendix.A of the main text, we should replace the 1 in the denominator of Eq.(S1) by the quasi-unit 1_{k^+} , and through the fluctuations in boundary between the k^+ -independent and k -independent segments, we have

$$\partial_k (1_{k^+} - \partial_k f_0) = \frac{(1 - \partial_k f_0) \partial_k f_0}{f_0}, \quad (\text{S9})$$

where $\partial_k 1_{k^+} = \frac{\partial_k f_0}{f_0}$ is the maximal possible k^+ -dependence of the lower boundary of the k^+ -independence segment due to the fluctuation, and $\partial_k 1_{k^+} = \frac{(\partial_k f_0)^2}{f_0}$.

B CALS of first set in terms of the the conserved quantity in the centroid

Here we present the analytical results for the conserved quantity $H_0 = I_0 - f_0$ at the local point of the centroid, i.e., the variable k . While around this centroid, we have the following correlations between local points, where arbitrarily two of them are correlated by a certain invariant relation (of the same party),

$$\begin{aligned}\lim_{k^- \rightarrow \infty} H_0 &= I_0 = \frac{H_0}{1 - \partial_k^- H_0} = \frac{I_0 - f_0}{1 - \frac{f_0}{I_0}}, \\ \lim_{k^- \rightarrow \infty} H_0 &= \frac{I_0 - f_0}{2f_0 - I_0} f_0 = \frac{H_0}{1 - \partial_k H_0} = \frac{I_0 - f_0}{1 - \frac{I_0 - f_0}{f_0}}, \\ \lim_{k \rightarrow \infty} H_0 &= f_0 - \frac{f_0^2}{I_0} = \frac{H_0}{1 - \partial_k^+ H_0} = \frac{I_0 - f_0}{1 - \frac{f_0 - I_0}{f_0}}.\end{aligned}\tag{S10}$$

We can obtain following relations: For H_0 :

$$\begin{aligned}\partial_k^- H_0 &= \frac{f_0}{I_0} = \frac{\partial_k f_0}{\partial_k f_0 - 1}, \\ \partial_k H_0 &= \frac{I_0 - f_0}{f_0} = \frac{-1}{\partial_k f_0}, \\ \partial_k^+ H_0 &= \frac{f_0 - I_0}{f_0} = \frac{1}{\partial_k f_0},\end{aligned}\tag{S11}$$

where they satisfy

$$\frac{\partial_k^+ H_0}{\partial_k H_0 \partial_k^- H_0} = \frac{-I_0}{f_0};\tag{S12}$$

For ratio $\frac{I_0}{f_0}$

$$\begin{aligned}\partial_k^- \frac{I_0}{f_0} &= \frac{2f_0 - I_0}{(f_0 - I_0)I_0}, \\ \partial_k \frac{I_0}{f_0} &= \frac{I_0}{f_0^2}, \\ \partial_k^+ \frac{I_0}{f_0} &= \frac{(2f_0 - I_0)I_0^2}{(f_0 - I_0)^2 f_0^2},\end{aligned}\tag{S13}$$

where they satisfy

$$\frac{\partial_k^+ \frac{I_0}{f_0}}{\partial_k \frac{I_0}{f_0} \partial_k^- \frac{I_0}{f_0}} = \frac{I_0^2}{f_0 - I_0}.\tag{S14}$$

For individual I_0 and f_0 ,

$$\begin{aligned}\partial_k^- I_0 &= \frac{f_0((f_0 - I_0)^2 + f_0^2)}{(f_0 - I_0)^2 I_0} = \frac{\partial_k f_0 + \partial_k f_0^3}{\partial_k f_0 - 1}, \\ \partial_k I_0 &= \frac{(2f_0 - I_0)I_0}{f_0(f_0 - I_0)} = \partial_k f_0 - \frac{1}{\partial_k f_0}, \\ \partial_k^+ I_0 &= \frac{I_0(-f_0^3 + 5f_0^2 I_0 - 4f_0 I_0^2 + I_0^3)}{f_0(f_0 - I_0)^3} = \frac{1}{\partial_k f_0} - \partial_k f_0 - (\partial_k f_0)^2 + (\partial_k f_0)^3,\end{aligned}\tag{S15}$$

with

$$\begin{aligned}\partial_k^- f_0 &= \frac{(\partial_k f_0)^3}{\partial_k f_0 - 1}, \\ \partial_k^+ f_0 &= -\partial_k f_0 - (\partial_k f_0)^2 + (\partial_k f_0)^3.\end{aligned}\tag{S16}$$

For this set, they always satisfy

$$\frac{\frac{\partial_k^+ \frac{I_0}{f_0}}{\partial_k^+ H_0}}{\frac{\partial_k \frac{I_0}{f_0} \partial_k^- \frac{I_0}{f_0}}{\partial_k H_0 \partial_k^- H_0}} = \frac{I_0 f_0}{I_0 - f_0}.\tag{S17}$$

The derivatives (by the next order) on different limiting scaled H_0 are

$$\begin{aligned}\partial_k^- \lim_{k^- \rightarrow \infty} H_0 &= \partial_k^- I_0 = \frac{\partial_k f_0 + \partial_k f_0^3}{\partial_k f_0 - 1}, \\ \partial_k \lim_{k^- \rightarrow \infty} H_0 &= \frac{-2f_0(f_0 - I_0)}{(I_0 - 2f_0)^2} = \frac{-2\partial_k f_0}{(1 + \partial_k f_0)^2}, \\ \partial_k^+ \lim_{k \rightarrow \infty} H_0 &= \frac{f_0}{I_0} \frac{f_0}{f_0 - I_0} = \frac{(\partial_k f_0)^2}{\partial_k f_0 - 1}.\end{aligned}\tag{S18}$$

The relation with the second set can be revealed by

$$\frac{\partial_{k^+} \lim_{k \rightarrow \infty} H_0}{\partial_{k^-} H_0} = \frac{1}{\partial_{k^+} H_0} = \partial_k f_0 = \frac{\partial_k I}{\partial_k f} = \frac{\partial I}{\partial f} = \frac{f}{I}, \quad (\text{S19})$$

where according to the definition illustrated in Eq.(S30), we have

$$\partial_k e^\alpha = \partial_k \frac{I}{\lim_{k \rightarrow \infty} H_0} = \frac{(\partial_k f_0)^2}{-f_0} = \frac{\partial_{k^+} \lim_{k \rightarrow \infty} H_0}{\lim_{k \rightarrow \infty} H_0}. \quad (\text{S20})$$

Here we note that, for second set, the derivatives with k in the numerator and denominator can be simply removed to obtain the derivative for I with f . But for the first set, to accessing

$$\frac{\partial_k I_0}{\partial_k f_0} = \frac{\partial I_0}{\partial f_0} = 1 - \frac{1}{(\partial_k f_0)^2}, \quad (\text{S21})$$

it requires

$$\frac{\partial}{\partial f_0} \ln \frac{1}{1 - \frac{1}{\partial_k f_0}} = \frac{-1}{f_0 \partial_k f_0}. \quad (\text{S22})$$

By letting $\delta = -\frac{1}{\partial_k f_0}$, we know there exists a scaling due to the cutoff,

$$\lim_{|\delta| \rightarrow 0} \ln \frac{1}{1 - \frac{1}{\partial_k f_0}} = \frac{1}{\partial_k f_0}, \quad (\text{S23})$$

which is consistent with the $\partial_k l_0 = \partial_k (l_0^{-1})^{-1} \rightarrow \frac{1}{\partial_k f_0}$. Thus there is a trisection configuration with these two sets. The above formula (Eq.(S19)) shows that the derivative on the infinitely scaled result of the target function f_0 by next order is related to the ratio between derivatives of H_0 by the neighbor orders. Similarly, for $I_0 = \lim_{k \rightarrow \infty} H_0$, we have $\partial_{k^-} I_0 = \frac{\partial_{k^-} H_0}{\partial_{k^-} H_0}$. after the necessary rescaling by exponential factor (similar to the ones described by Eq.(S23,S21), the I_0 in the first block of the first set, could satisfy

$$\frac{\partial_k \lim_{k \rightarrow \infty} H_{00}}{\partial_{k^-} H_{00}} = \frac{1}{\partial_k H_{00}} = \partial_{k^-} f_{00} = \frac{\partial_{k^-} I_0}{\partial_{k^-} f_0} = \frac{\partial I_0}{\partial f_0} \frac{f_0}{I_0}, \quad (\text{S24})$$

where f_{00} is another target function ($H_{00} = I_{00} - f_{00}$) and satisfies

$$\begin{aligned} I_0 &= e^\beta \lim_{k \rightarrow \infty} f_{00}, \\ f_0 &= I_0 \partial_{k^-} f_{00}, \\ \partial_{k^-} e^\beta &= \frac{(\partial_{k^-} f_{00})^2}{-f_{00}}. \end{aligned} \quad (\text{S25})$$

Since in the absence of stretching, we have

$$\partial_k \ln(-1) = \partial_k \ln(-f_0) - \partial_k \ln(1 - \partial_k f_0), \quad (\text{S26})$$

and consistently,

$$\partial_k \ln(-1) - \partial_k \ln[\lim_{k \rightarrow \infty} H_0] = \partial_k \ln(-1) - \partial_k \ln \frac{-f_0}{1 + \partial_k f_0} = \partial_k \ln \frac{1 + \partial_k f_0}{1 - \partial_k f_0}. \quad (\text{S27})$$

By substituting solution in Eq.(S18), we have

$$\partial_k \left(\frac{\partial_k f_0 + 1}{\partial_k f_0 - 1} \right) = \frac{-2}{I_0}, \quad (\text{S28})$$

which is valid as long as $\partial_k \ln(-1)$ is be estimated as zero, like in Eqs.(S26,S27). The value of this term will be changed once $\partial_k \ln(-1)$ be endowed a finite value, as we show in the next section.

C Second set of CALS: cutoff-independent CALS

From the first expression in the first set of CALS (Eq.(S10)), and combined with the discussion in above section, we know

$$\begin{aligned} \lim_{k \rightarrow \infty} I_0 &= I_0, \\ \lim_{k \rightarrow \infty} f_0 &= 0, \end{aligned} \quad (\text{S29})$$

where the first result means I_0 is independent with $k \rightarrow \infty$ and this in fact determines the cutoff of the $\{k\}$ -dependence in the first set of CALS, and correspondingly, such cutoff determines the maximal upper limit of the nonzero series

summation in f_0 , which is proportional to the power of $\partial_k f_0$. Now we introduce the second set of the CALS where we define the conserved quantity in the centroid as $h = (I - f)$,

$$\lim_{k^- \rightarrow \infty} h = I = \frac{I - f}{1 - \partial_k h} = \frac{I - f}{1 - \frac{f}{I}}, \quad (\text{S30})$$

Similar to the first set, here we also have $I = f \frac{\partial_k f^{-1}}{\partial_k f}$. The most prominent characteristic for the variables in this set (I, f) , comparing to that of the first set $((I_0, f_0))$, is the following relation,

$$\begin{aligned} \frac{f}{I} &= \frac{\partial_k I}{\partial_k f} = \frac{\partial_k f}{\partial_k f - 1} = \partial_k f_0, \\ \partial_k f &= \frac{f}{f - I} = \partial_k^- H_0 = \frac{\partial_k f_0}{\partial_k f_0 - 1}. \end{aligned} \quad (\text{S31})$$

where I is related to the H_0 in Eq.(S10) by

$$\partial_k I = \partial_{k^+} \left(\lim_{k \rightarrow \infty} H_0 \right) = \partial_{k^+} \left(\lim_{k \rightarrow \infty} f_0 \right) = \frac{\partial_k^- H_0}{\partial_{k^+} H_0} = \frac{f}{I} \frac{f}{f - I} = \frac{(\partial_k f_0)^2}{\partial_k f_0 - 1}, \quad (\text{S32})$$

where we can then extend the expression in Eq.(50) to

$$\frac{\partial \mathbf{I}[\mathbf{p} + k]}{\partial k} = \frac{\partial \mathbf{I}[\mathbf{p} + k^+]}{\partial k^+} = \frac{\partial \mathbf{I}[\mathbf{p}]}{\partial \mathbf{p}}, \quad (\text{S33})$$

where we regard I as one of the action in the k^- -independent segment $\mathbf{I}[\mathbf{p} + k]$, but indeed this reflects a nonlocal symmetry property. This can be seen from the actual expressions of the I and f , which can be obtained from Eq.(S32),

$$\begin{aligned} I &= \frac{-\partial_k f_0 (\partial_k f_0 + 1)}{\partial_k^{(2)} f_0}, \\ f &= \frac{-(\partial_k f_0)^2 (\partial_k f_0 + 1)}{\partial_k^{(2)} f_0}, \end{aligned} \quad (\text{S34})$$

where the relations Eq.(S31,S32) can be verified in terms of the above expressions, and there are several derivatives used here, which in terms of (I, f) reads

$$\begin{aligned} \partial_k f_0 &= \frac{f}{I}, \\ \partial_k^{(2)} f_0 &= \frac{f}{I(f - I)} \left(1 - \frac{f^2}{I^2} \right) = -\frac{\partial_k f_0 (1 + \partial_k f_0)}{I}, \\ \partial_k^{(3)} f_0 &= \frac{\partial_k f_0 (-1 - 2\partial_k f_0 + 2(\partial_k f_0)^2 + 3(\partial_k f_0)^3)}{(\partial_k f_0 - 1)I^2}, \end{aligned} \quad (\text{S35})$$

Since, as we mention before, the variables of the second set show more the nonlocal characteristic instead of the local one, e.g., from Eq.(S33), it seems its functional derivative (or the corresponding action) only reveals the maximal boundary-fluctuation-induced nonzero functional derivative, among all the segments above the cutoff. Also, from Eq.(S34), we found it contains first order and second order derivative of f_0 , with respect its corresponding variable k , which is also the centroid of the group $\{k\}$ in this system. To figure out more clearly the relation between the two sets and the role played by the second set, we compare the two derivatives on the first order derivative $\partial_k f_0$: From the third expression of Eq.(S19), we can obtain

$$\partial_{k^+} (\partial_k f_0) = \partial_{k^+} \frac{f}{I} = \frac{\partial_k f_0 - (\partial_k f_0)^2 - (\partial_k f_0)^3 + (\partial_k f_0)^4}{f_0}. \quad (\text{S36})$$

Comparing this expression to one in the second line of Eq.(S39), which is equivalent to $\partial_k \frac{f}{I}$. To see the potential global feature in the second set, we now let $k \approx k^+ \rightarrow \infty$, in which case we now have

$$\tilde{I} = -\frac{f_0}{(\partial_k f_0 - 1)^2}, \quad (\text{S37})$$

where the $|$ is approximated to form that depends only on the first order derivative $\partial_k f_0$, correspondently,

$$\tilde{f} = -\frac{f_0 \partial_k f_0}{(\partial_k f_0 - 1)^2}. \quad (\text{S38})$$

Then the Eq.(S39) can be written as

$$\begin{aligned} \partial_k f_0 &= \frac{\tilde{f}}{\tilde{I}}, \\ \partial_k^{(2)} f_0 &= \frac{(\partial_k f_0 - 1)^2 \partial_k f_0 (1 + \partial_k f_0)}{f_0}, \\ \partial_k^{(3)} f_0 &= \frac{(\partial_k f_0 - 1)^3 \partial_k f_0 (1 + \partial_k f_0) (-1 - \partial_k f_0 + 3(\partial_k f_0)^2)}{f_0^2}, \end{aligned} \quad (\text{S39})$$

Then there are two and only two solutions for the derivative $\partial_k f_0$, which satisfy that the value of $(-h)$ equals to all the three limit results in Eq.(S18) of the first set, which reveals an overall CALS, instead of just one or two (adjacent) of the variable,

$$\begin{aligned} -\tilde{h} = -(\tilde{I} - \tilde{f}) &= \lim_{k \rightarrow -\infty} H_0 + \lim_{k \rightarrow -\infty} H_0 + \lim_{k \rightarrow \infty} H_0 = \frac{f_0}{1 - \partial_k f_0} + \frac{f_0(I_0 - f_0)}{2f_0 - I_0} + I_0 \\ &= \frac{(1 - \partial_k f_0 - 3(\partial_k f_0)^2 + (\partial_k f_0)^3)f_0}{\partial_k f_0((\partial_k f_0)^2 - 1)}, \end{aligned} \quad (\text{S40})$$

which are the golden ratio $\partial_k f_0 = \frac{\pm\sqrt{5}+1}{2}$. In fact, the golden ratio has also proved to be related to the quantum chaos in the thermalization limit[1, 2], and the appearance of golden ratio here is not a coincidence. We also found that, there are three and only three solutions for the derivative $\partial_k f_0$, that satisfy

$$\tilde{I} = \left(\lim_{k \rightarrow -\infty} H_0 - f_0 \right) + \lim_{k \rightarrow -\infty} H_0 + \lim_{k \rightarrow \infty} H_0 = \frac{f_0}{1 - \partial_k f_0} + \frac{f_0(I_0 - f_0)}{2f_0 - I_0} + I_0 - f_0, \quad (\text{S41})$$

which are $\partial_k f_0 = \frac{\pm\sqrt{5}+1}{2}, \frac{1}{3}$.

The special role for these three solutions can be further verified in terms the ansatz of the delta-function-type, where we use the recurrenion relations between the derivatives of the delta-function. For $\partial_k f_0 = \frac{\sqrt{5}+1}{2}$,

$$\begin{aligned} \partial_k f_0 &= \delta^{(1)}(x) = \frac{-1}{x} \delta(x) = 1.61803, \\ \partial_k^{(2)} f_0 &= \frac{\delta^{(1)}(x)}{\delta(x)} = \frac{-1}{x} = \frac{1.61803}{f_0}, \\ \partial_k^{(3)} f_0 &= \frac{\delta^{(2)}(x)}{\delta(x)} = \frac{2}{x^2} = \frac{5.23607}{f_0^2}, \\ \partial_k^{(4)} f_0 &= \frac{\delta^{(3)}(x)}{\delta(x)} = \frac{-6}{x^3} = \frac{25.4164079}{f_0^3}, \end{aligned} \quad (\text{S42})$$

where $\delta(x) = f_0$; which is compatible with the result given by the golden ratio,

$$\phi_g = 1.61803, \quad 2\phi_g^2 = 5.23606797, \quad 6\phi_g^3 = 25.4164079. \quad (\text{S43})$$

Thus the correspondence between the derivatives $\partial_k f_0$ and the ratios between the derivative of delta-type function and itself can be verified, and it is strictly predicted by the golden ratio until the fourth order, $\partial_k^{(4)} f_0$. But note that all the derivative within Eq.(S42) the replacement of I in Eq.(S34) by the \tilde{I} in Eq.(S37) should be done only after the derivatives on f_0 as well as I . More mysteriously, for the fourth order one, $\partial_k^{(4)} f_0$, which is the term just before the valid prediction of golden ratio disappear, we found that, there is a gradual change on the k -dependence of each I within a multiple of I , which is

$$\begin{aligned} \partial_k I &= Eq.(S32), \\ \partial_k I^2 &= I\partial_k I + I(\partial_k I + \frac{1}{2} \frac{f_0}{\tilde{I}}). \end{aligned} \quad (\text{S44})$$

For $\partial_k f_0 = \phi'_g = \frac{-\sqrt{5}+1}{2}$,

$$\begin{aligned} \partial_k f_0 &= \delta^{(1)}(x') = \frac{-1}{x'} \delta(x') = -0.618034, \\ \partial_k^{(2)} f_0 &= \frac{\delta^{(1)}(x')}{\delta(x')} = \frac{-1}{x'} = \frac{-0.618034}{f_0}, \\ \partial_k^{(3)} f_0 &= \frac{\delta^{(2)}(x')}{\delta(x')} = \frac{2}{x'^2} = \frac{0.763932}{f_0^2}, \\ \partial_k^{(4)} f_0 &= \frac{\delta^{(3)}(x')}{\delta(x')} = \frac{-6}{x'^3} = \frac{-1.41640786}{f_0^3}, \end{aligned} \quad (\text{S45})$$

which is compatible with the result given by the golden ratio,

$$\phi'_g = -0.618034, \quad 2\phi_g'^2 = 0.7639320225, \quad 6\phi_g'^3 = -1.41640786, \quad (\text{S46})$$

and the Eq.(S44) is still valid here.

For $\partial_k f_0 = \frac{1}{3}$,

$$\begin{aligned} \partial_k f_0 &= \frac{1}{3} \\ \partial_k^{(2)} f_0 &= \frac{0.197531}{f_0}, \\ \partial_k^{(3)} f_0 &= \frac{0.131687}{f_0^2}, \\ \partial_k^{(4)} f_0 &= \frac{0.117055}{f_0^3}, \end{aligned} \quad (\text{S47})$$

where

$$\frac{\partial_k^{(3)} f_0}{\partial_k^{(2)} f_0} = \frac{1 - \partial_k f_0}{f_0} = \frac{2}{3} \frac{1}{f_0}, \quad (\text{S48})$$

and furthermore, using the formular for the second and third order delta-function derivatives

$$\begin{aligned} \delta^{(2)}(x) &= \frac{2(\partial_k f_0)^2}{f_0} = \frac{2}{3} \frac{\partial_k f_0}{f_0}, \\ \delta^{(3)}(x) &= \frac{6(\partial_k f_0)^3}{f_0^2} = \frac{2}{3} \frac{\partial_k f_0}{f_0^2}, \end{aligned} \quad (\text{S49})$$

and the above derivative in Eq.(S47) can be predicted by the value of $\partial_k f_0$ in terms of the recurrenction relations until the fourth order,

$$\begin{aligned} 4[\partial_k f_0(1 - \partial_k f_0)]^2 &= 0.1975308641975, \\ 12[\partial_k f_0(1 - \partial_k f_0)]^3 &= 0.131687243, \\ 48[\partial_k f_0(1 - \partial_k f_0)]^4 &= 0.117055327, \end{aligned} \quad (\text{S50})$$

and different to the cases with golden ratio, there is another gradual change on the k -dependence of each I within a multiple of it, which is

$$\partial_k I^2 = I \partial_k I + I(\partial_k I - \frac{f_0}{I}). \quad (\text{S51})$$

Comparing to Eq.(S44), and by treating the individual I within the multiple as the few body operators of the same symmetry sector, the smaller variance (inversely proportional to the fluctuation between distinct values) of their k -derivative shows the further enhanced nonlocal conservation compared to the above case with golden ratio. And such nonlocal symmetry is directly related to the limit where $\partial_k \approx \partial_{k+}$

Thus the case for $\partial_k f_0 = \frac{1}{3}$ is different from the cases where $\partial_k f_0$ equals the Golden ratio. The parameter $\frac{1}{3}$ together with the Golden ratio also appear in the contents about the ETH diagnosis, e.g., in the non-thermal systems which may be induced by the nonlocal correlations. In one-dimensional non-Abelian anyon chains[4] or the Rydberg atoms chains[3] with constrained Hilbert space, whose dimension scale as $(\frac{1+\sqrt{5}}{2})^L$ with L the system size, previous studies[3, 5] found that the number density of a single local site equals $\frac{1}{3}$, instead of the value predicted in the Gibbs ensemble with ETH, which is $(1 + (\frac{1+\sqrt{5}}{2})^2)^{-1}$.

But note that all three cases appear in this section are of the integrable nonergodic limit, due to the large fluctuation in the boundaries between arbitrarily two segments. Further, unlike the first set of CALS, the second set of CALS does not rely on the finite cutoff (order of derivative $\partial_k f_0$ to generate nonlocal symmetries), by the aid of special "nonlocal" quantity I , and the term $h = (I - f)$ has the following values

$$\begin{aligned} h = I - f &= \frac{\sqrt{5} + 1}{2} f_0, \\ h = I - f &= -\frac{\sqrt{5} + 1}{2} f_0, \\ h = I - f &= -\frac{3}{2} f_0, \end{aligned} \quad (\text{S52})$$

for $\partial_k f_0 = \frac{\sqrt{5}+1}{2}$, $-\frac{\sqrt{5}+1}{2}$ and $\frac{1}{3}$, respectively.

D delta-function approximation and the cutoff of the first set of CALS

Firstly we recall the second derivative of f_0 , in the presence of of finite IR cutoff,

$$\partial_k^{(2)} f_0 = (\partial_k f_0 - 1) \frac{\partial_k f_0}{f_0}. \quad (\text{S53})$$

The cutoff indeed plays the role of $\ln(-1)$ terms here. To see this, we rewrite the Eq.(2) as (including the effective $\ln(-1)$ terms now)

$$\frac{\partial_k f_0}{-f_0} = \partial_k \ln \frac{1}{1 - \partial_k f_0} = \partial_k \left[\frac{1}{1 - \partial_k f_0} \left(\frac{\partial}{\partial(\partial_k f_0)} \right)^{-1} \right] = \partial_k \delta, \quad (\text{S54})$$

where $\delta = \left(\frac{\partial}{\partial(\partial_k f_0)} \right)^{-1} = -\partial_k f_0$, with the corresponding target length $l_0^{-1} = \frac{\partial_k \delta}{\delta} = f_0^{-1}$. The existence of nonzero $\ln(-1)$ terms and teh intrinsic properties for a well-defined delta-type function results in the scaling

$$\delta = (1 - \partial_k f_0) \ln \frac{1}{1 - \partial_k f_0} \rightarrow -\partial_k f_0, \quad (\text{S55})$$

where the expression before scaling is in the form of von Neumann entropy, and describes the definition of δ at the moment followed by the isolation of operator $\frac{\partial}{\partial(\partial_k f_0)}$ with $\text{Li}_1(\partial_k f_0) = \ln \frac{1}{1-\partial_k f_0}$. While the form after scaling reflect the δ defined according to its dependence with variable k . At this stage, we have

$$\frac{\partial_k \ln(-1)}{\partial_k(-\delta)} = \frac{1}{f_0 \partial_k(-\delta)} - \frac{1}{-\delta}. \quad (\text{S56})$$

To detecting more properties, we next cancel the dependence with common variable k , by scaling it to a certain value ($< \infty$) to make $|\partial_k f_0| = |-\delta| \rightarrow 0$, then we have

$$\delta^{-1} \frac{\partial \delta}{\partial x} = \frac{-1}{x}, \quad (\text{S57})$$

where $x := \frac{\delta}{\delta - e^\delta}$. This is obtained from the the previous expression,

$$\delta^{-1} \frac{\partial_k \delta}{\partial_k \ln \frac{1}{1-\partial_k f_0}} = \frac{1 - \partial_k f_0 - \delta}{\delta}, \quad (\text{S58})$$

where $\text{Li}_1(\partial_k f_0) = \ln \frac{1}{1-\partial_k f_0} \rightarrow \partial_k f_0$ by letting $|\partial_k f_0| = \partial_k f_0 e^{-i \text{Arg} \partial_k f_0} \rightarrow 0$. In the mean time, this results in the above definition of x . Now the target variable becomes x instead of k .

The strict cutoff nature for the delta function leads to

$$\begin{aligned} x^2 \frac{\partial \delta}{\partial x} &= 0, \\ \int_{-1}^1 dx \delta\left(\frac{1}{x}\right) &= 0. \end{aligned} \quad (\text{S59})$$

As we know the scaling in above formula has $|-\delta| = 0^+$, thus to using this property, we need to modifies teh first formula to the form $x^2 \frac{\partial \delta}{\partial x} = 0^+$. This can be done by using the second formula, where we can obtain

$$\int_{-1}^1 dx \delta\left(\frac{1}{x}\right) = \int_{-1}^1 dx \frac{\partial \delta(\frac{1}{x})}{\partial \frac{1}{x}} x = [\delta(\frac{1}{x})x]_{-1}^1 - \int_{-1}^1 d\left(\frac{1}{x}\right) \delta\left(\frac{1}{x}\right) (-x^2) = x^2 \frac{\partial \delta}{\partial x} = 0. \quad (\text{S60})$$

Since the first term in above formula has

$$[\delta(\frac{1}{x})x]_{-1}^1 = \int_{-1}^1 [x \frac{\partial}{\partial \frac{1}{x}} \delta(\frac{1}{x}) - x^2 \delta(\frac{1}{x})], \quad (\text{S61})$$

the above cutoff at $\int_{-1}^1 dx \delta(\frac{1}{x}) = 0$ indeed corresponds to cutoff at $x \frac{\partial}{\partial \frac{1}{x}} = 0$. Thus a finite value of $x^2 \frac{\partial \delta}{\partial x} = 0^+$ can be realized by endowing $x \frac{\partial}{\partial \frac{1}{x}} \delta(\frac{1}{x})$ a value.

Now we focus on the first term of above formula, which can be reformed into

$$[\delta(\frac{1}{x})x]_{-1}^1 = \int_{-1}^1 d\left[\frac{1}{x} [-\delta(\frac{1}{x})]\right] = \int d\Delta \frac{\partial x^2}{\partial \Delta} \frac{\partial \delta}{\partial x} = [x^2 \frac{\partial \delta}{\partial x}]_{\Delta_2}^{\Delta_1} - \int x^2 \frac{\partial}{\partial \Delta} \left(\frac{\partial \delta}{\partial x}\right). \quad (\text{S62})$$

Relating this to the Eq.(S60), we have the following relations where the limits are reached spontaneously

$$\begin{aligned} [x^2 \frac{\partial \delta}{\partial x}] &= 0 \rightarrow [x^2 \frac{\partial \delta}{\partial x}]_{\Delta_2}^{\Delta_1} = 0^+, \\ \int_{-1}^1 \delta\left(\frac{1}{x}\right) (-x^2) d\left(\frac{1}{x}\right) &\rightarrow - \int x^2 \frac{\partial}{\partial \Delta} \left(\frac{\partial \delta}{\partial x}\right) d\Delta = \frac{-1}{2} [x^2 \frac{\partial \delta}{\partial x}]_{\Delta_2}^{\Delta_1} = \frac{-1}{2} 0^+, \\ \int_{-1}^1 [x \frac{\partial}{\partial \frac{1}{x}} \delta(\frac{1}{x})] d\left(\frac{1}{x}\right) &= -2 \int_{-1}^1 \delta\left(\frac{1}{x}\right) (-x^2) d\left(\frac{1}{x}\right) \rightarrow 2 \int x^2 \frac{\partial}{\partial \Delta} \left(\frac{\partial \delta}{\partial x}\right) d\Delta, \\ [\delta(\frac{1}{x})x]_{-1}^1 &= \int_{-1}^1 \delta\left(\frac{1}{x}\right) (x^2) d\left(\frac{1}{x}\right) \rightarrow \int d\Delta \frac{\partial x^2}{\partial \Delta} \frac{\partial \delta}{\partial x}. \end{aligned} \quad (\text{S63})$$

Thus we have

$$\begin{aligned} d\left(\frac{1}{x}\right) &= \frac{1}{\delta(\frac{1}{x})} \frac{\partial}{\partial \Delta} \left(\frac{\partial \delta}{\partial x}\right) d\Delta, \\ &= \frac{1}{\delta(\frac{1}{x})} \frac{1}{x^2} \frac{\partial x^2}{\partial \Delta} \frac{\partial \delta}{\partial x} d\Delta, \end{aligned} \quad (\text{S64})$$

where we have

$$\begin{aligned} d\left(\frac{1}{x}\right) &= \frac{1}{-\delta(\frac{1}{x})} \frac{\partial x^2}{\partial \Delta} \frac{\partial \delta}{\partial x} d\Delta \\ &= \frac{1}{\delta(\frac{1}{x})} \frac{\partial}{\partial \Delta} \left(\frac{\partial \delta}{\partial x}\right) d\Delta = \left[\frac{\partial \frac{1}{x}}{\partial \Delta}\right] d\Delta. \end{aligned} \quad (\text{S65})$$

And we can obtain

$$\begin{aligned} \frac{\partial_{\Delta}(\frac{\partial\delta(x)}{\partial x})}{\frac{\partial\delta(x)}{\partial x}} &= \frac{1}{x^2} \frac{\partial x^2}{\partial \Delta} = \frac{-1}{X_2}, \\ \partial_{\Delta} \ln(-\delta(x)) &= \frac{\partial_{\Delta}(-\delta(x))}{-\delta(x)} = x \frac{\partial \frac{1}{x}}{\partial \Delta} \left[-\frac{\delta(\frac{1}{x})}{\delta(x)} - 1 \right] = \frac{-1}{X_3}, \end{aligned} \quad (\text{S66})$$

where the target variables read

$$\begin{aligned} X_2 &= \left[\frac{-1}{x^2} \frac{\partial x^2}{\partial \Delta} \right]^{-1}, \\ X_3 &= \left(x \frac{\partial \frac{1}{x}}{\partial \Delta} \left[\frac{\delta(\frac{1}{x})}{\delta(x)} + 1 \right] \right)^{-1}, \end{aligned} \quad (\text{S67})$$

and the Δ_1 and Δ_2 defined according to

$$\begin{aligned} \lim_{\Delta \rightarrow X_2 = \Delta_1} X_2^2 \partial_{\Delta} \left(\frac{\partial \delta(x)}{\partial x} \right) &= 0, \\ \lim_{\Delta \rightarrow X_3 = \Delta_2} X_3^2 \partial_{\Delta} (-\delta(x)) &= 0. \end{aligned} \quad (\text{S68})$$

References

- [1] Mondaini, Rubem, and Marcos Rigol. "Many-body localization and thermalization in disordered Hubbard chains." *Physical Review A* 92.4 (2015): 041601.
- [2] Li, Xiao, Xiaopeng Li, and S. Das Sarma. "Mobility edges in one-dimensional bichromatic incommensurate potentials." *Physical Review B* 96.8 (2017): 085119.
- [3] Lin, Cheng-Ju, and Olexei I. Motrunich. "Exact quantum many-body scar states in the Rydberg-blockaded atom chain." *Physical review letters* 122.17 (2019): 173401.
- [4] Chandran, A., Marc D. Schulz, and F. J. Burnell. "The eigenstate thermalization hypothesis in constrained Hilbert spaces: A case study in non-Abelian anyon chains." *Physical Review B* 94.23 (2016): 235122.
- [5] Lin, Cheng-Ju, Anushya Chandran, and Olexei I. Motrunich. "Slow thermalization of exact quantum many-body scar states under perturbations." *Physical Review Research* 2.3 (2020): 033044.
- [6] Tasaki, Hal. "Typicality of thermal equilibrium and thermalization in isolated macroscopic quantum systems." *Journal of Statistical Physics* 163 (2016): 937-997.
- [7] Moudgalya, Sanjay, et al. "Exact excited states of nonintegrable models." *Physical Review B* 98.23 (2018): 235155.
- [8] Canovi, Elena, et al. "Quantum quenches, thermalization, and many-body localization." *Physical Review B* 83.9 (2011): 094431.
- [9] Cecile, Guillaume, Jacopo De Nardis, and Enej Ilievski. "Squeezed ensembles and anomalous dynamic roughening in interacting integrable chains." *Physical Review Letters* 132.13 (2024): 130401.
- [10] Cheng, Jun-Qing, Shuai Yin, and Dao-Xin Yao. "Dynamical localization transition in the non-Hermitian lattice gauge theory." *Communications Physics* 7.1 (2024): 58.
- [11] Popescu, Sandu, Anthony J. Short, and Andreas Winter. "Entanglement and the foundations of statistical mechanics." *Nature Physics* 2.11 (2006): 754-758.
- [12] Shiraishi, Naoto, and Takashi Mori. "Systematic construction of counterexamples to the eigenstate thermalization hypothesis." *Physical review letters* 119.3 (2017): 030601.
- [13] Karamlou, Amir H., et al. "Probing entanglement in a 2D hard-core Bose-Hubbard lattice." *Nature* (2024): 1-6.
- [14] Maki, Jeff, and Fei Zhou. "Signatures of Conformal Symmetry in the Dynamics of Quantum Gases: A Cyclic Quantum State and Entanglement Entropy." *arXiv preprint arXiv:2404.15827* (2024).
- [15] Turner, Christopher J., et al. "Weak ergodicity breaking from quantum many-body scars." *Nature Physics* 14.7 (2018): 745-749.
- [16] Choi, Soonwon, et al. "Emergent SU(2) dynamics and perfect quantum many-body scars." *Physical review letters* 122.22 (2019): 220603.
- [17] Moise, Abed Alsalam Abu, Graham Cox, and Marco Merkli. "Entropy and entanglement in a bipartite quasi-Hermitian system and its Hermitian counterparts." *Physical Review A* 108.1 (2023): 012223.
- [18] Shao, Kai, et al. "Non-Hermitian Moiré Valley Filter." *Physical Review Letters* 132.15 (2024): 156301.
- [19] Sandvik, Anders W., and Hans Gerd Evertz. "Loop updates for variational and projector quantum Monte Carlo simulations in the valence-bond basis." *Physical Review B* 82.2 (2010): 024407.
- [20] Srednicki, Mark. "Chaos and quantum thermalization." *Physical review e* 50.2 (1994): 888.
- [21] Deutsch, Joshua M. "Eigenstate thermalization hypothesis." *Reports on Progress in Physics* 81.8 (2018): 082001.

- [22] Guhr, Thomas, Axel Müller–Groeling, and Hans A. Weidenmüller. "Random-matrix theories in quantum physics: common concepts." *Physics Reports* 299.4-6 (1998): 189-425.
- [23] Bohigas, Oriol. *Random matrix theories and chaotic dynamics*. No. IPNO-TH-90-84. Paris-11 Univ., 1991.
- [24] M. L. Mehta, "Random Matrices", (Elsevier, Amsterdam, 1991)
- [25] Borgonovi, Fausto, et al. "Quantum chaos and thermalization in isolated systems of interacting particles." *Physics Reports* 626 (2016): 1-58.
- [26] Haake, Fritz. *Quantum signatures of chaos*. Springer US, 1991.